
MULTISTEP MULTIAPPLIANCE LOAD PREDICTION

A PREPRINT

Alona Zharova*
Humboldt-Universität zu Berlin
Berlin, Germany
alona.zharova@hu-berlin.de

Antonia Scherz
Humboldt-Universität zu Berlin
Berlin, Germany
antonia.scherz@hu-berlin.de

December 20, 2022

ABSTRACT

A well-performing prediction model is vital for a recommendation system suggesting actions for energy-efficient consumer behavior. However, reliable and accurate predictions depend on informative features and a suitable model design to perform well and robustly across different households and appliances. Moreover, customers' unjustifiably high expectations to accurate predictions may discourage them from using the system in the long-term. In this paper, we design a three-step forecasting framework to assess predictability, engineering features, and deep learning architectures to forecast 24 hourly load values. First, our predictability analysis provides a tool for expectation management to cushion customers' anticipations. Second, we design several new weather-, time- and appliance-related parameters for the modeling procedure and test their contribution to the model's prediction performance. Third, we examine six deep learning techniques and compare them to tree- and support vector regression benchmarks. We develop a robust and accurate model for the appliance-level load prediction based on four datasets from four different regions (US, UK, Austria, and Canada) with an equal set of appliances. The empirical results show that cyclical encoding of time features and weather indicators alongside a long-short term memory (LSTM) model offer the optimal performance.

Keywords Multivariate · Multistep · Time Series · Prediction · Appliance Level · Electricity Load

1 Introduction

Soaring energy costs and awareness of personal responsibility to reduce carbon emissions, especially in Europe [European Commission, 2021], fuel demand for reliable and detailed energy profiling. Recommender systems that visualize upcoming costs and carbon emissions rely on energy consumption forecasts. Thus, reliable prediction of daily appliance energy profiles with hourly consumption values facilitates consumers' and technologies' endeavors towards a sustainable everyday life.

Appliance load modeling suffers from high volatility and uncertainty in underlying data. Reliable and accurate predictions depend on informative features and a suitable model design to perform well and robustly across different households and appliances. Further, efficient prediction parameters largely depend on the time horizon and forecast granularity of the prediction problem. Deep learning addresses these challenges by efficiently processing highly variable data sources and flexibly adapting to large feature dimensions.

Many smart home applications in the private sector struggle with interoperability, usability and satisfying consumer expectations [International Energy Agency, 2018]. Especially preset and high expectations to fast response time and accurate prediction outcomes demand for quick responses and transparent results of forecasters, as well as direct expectation management to cushion anticipations. Additionally, prediction frameworks should produce reliable results to support smart home- or recommendation applications. This study, therefore, designs a three-step forecasting framework assessing the predictability of underlying data, verifying potent feature groups and evaluating reliable modeling architectures for the day ahead device level load profiling in one-hour time intervals.

*Correspondence author.

Until recently, existing approaches failed to simultaneously capitalize on additional information sources and efficient modeling structures. Comparative studies evaluate the predictability of appliance data leaving out an assessment of model performances on multistep forecasting tasks. Statistical approaches rely on separately modeling appliance on/off states and usage duration, while they fall short of reporting exact hourly usages. Most frameworks prove efficiency only in an aggregated setting for multiple appliances. Deep learning solutions concentrate on shorter prediction periods covering one hour ahead and higher data resolutions in minutes. Presented approaches fail to formulate longer (practical) forecasting horizons and largely ignore the potential lying in additional feature engineering.

This work addresses these shortcomings by setting up a suitable prediction problem of forecasting the next 24 hourly load values of typical appliances with different usage structures (i.e., fridge, washing machine, dryer, dishwasher, and television). The presented three-step framework evaluates data predictability, the impact of feature engineering and the performance of deep learning architectures across four different data sets from different geographical regions. Analyzed feature groups include additional information (environmental, date-time and appliance features) as well as engineered features using auto-correlation, statistical summary and phase space reconstruction techniques. Suitable model architectures includes new and existing approaches applied to related load prediction tasks. Inter alia the convolutional-long short-term memory network (CNN-LSTM) and sequence-to-sequence with a decoder learning a reversed feature representation (S2S reversed) architectures, as well as the multistep support vector regression (MSVR) are applied to device level prediction for the first time. The code for the proposed prediction framework is available on GitHub.

The remainder of this paper is organized as follows: The subsequent subsection provides an overview of related literature. Section 3 introduces the feature engineering and prediction methods as well as evaluation metrics. Section 4 presents the datasets, preprocessing and experimental design. Section 5 shows the results of the different prediction methods and analyzes their implications, while their limitations and an outlook on future research follow in section 6. Finally, section 7 concludes the presented work.

2 Related Literature

Modeling aggregated residential energy consumption has been studied extensively with large success. However, few studies look at individual appliance load profiles. Despite similarities in types of prediction problems and applicable forecasting methods, individual device load forecasts are much more susceptible to uncertainty from human usage decisions. Without aggregation, as in household level (aggregated) load forecasting, random estimation errors do not cancel each other out. Additionally, individual appliances more selectively depend on influential factors such as environmental conditions or time factors. Table 2.1, therefore, summarizes existing work on individual appliance level load predictions and applied features.

In detail, initial work modeling appliance electric profiles originates from bottom-up aggregated load profiling. Caspasso et al. [1994] analyze socioeconomic and demographic characteristics as well as average load profiles of household appliances from survey data and field measurements utilizing probability functions and a Monte Carlo extraction process. Paatero and Lund [2006] expanded this approach by formulating stochastic processes looking at collections of appliances from Finish households, separately simulating the use of each appliance.

With the advancement of data collection technologies, the most recent works build on more precise and larger datasets. Statistical approaches often indirectly estimate device-level electric consumption by modeling finite sets of operating states and the operating duration within each state to derive total load consumption profiles. Following this approach, Jin et al. [2020] utilize past on and off states for statistical analysis and probability simulations of daily television profiles. In Gao et al. [2018]’s work external environmental factors, time indicators and family internal characteristics identify similar past load patterns to resemble future patterns. A more complex approach in Ji et al. [2020] models operating states and duration times through K-means clustering combined with random sampling from state-specific probability distributions fed to a Conditional Hidden Semi-Markov model. The latter two studies predict aggregated values for groups of similar appliances.

In contrast, Singh and Yassine [2018] use a more data storage-intensive approach to profiling appliances. Based on frequent appliance usage patterns stored in an incrementally updated Database Management System their Bayesian Network predicts appliance activity. To derive total load consumption profiles for various time periods (hour, day, week, etc.), they combine the predicted activity state with the average appliance electric usage and operating duration.

These indirect and empirical methods highly depend on the frequency of observations, which increases the importance of frequently observed and former values over more recent load values less frequently observed. This leads to the lagged response problem, where sudden changes in appliance usage profiles influence predictions only after a certain

Table 2.1: Literature on Appliance Level Load Prediction

Authors	Dataset	Data Resolution	Target length (resolution)	Included Features	Multistep	Included Models	Best Model	Evaluation/ Performance
Capasso et al. (1994)	data surveys, average appliance usage	15 min	1 hour (aggregated appliances)	appliances (states, duration, usage), home members (age, gender), demographic information	yes	-	Monte Carlo extraction procedure and daily-use probability of appliances	Normalized Variation Factor (NVF) Day: 0.0801 $\geq NVF \geq 0.0220$
Paatero and Lund (2006)	Finnish home data, appliances	1 h	1 (hour/cycle length)	season, daily activity, social random factor	-	-	Starting Probability (from features) initiates mean consumption cycle	Deviation of mean (hourly): $\leq 5\%$
Lachut et al. (2014)	GreenHomes dataset	1 h/d/w	1 (hour/day/week)	time-of-day	no	KNN ¹ , bayesian predictor, SVM ² , - ARMA ³ , naive model	-	95% accuracy fridge (hourly/daily): 89%/74%
Gao et al. (2018)	not specified	10 min	1440 (24 h)	weather, events, date, time, sociological variables	yes	Mean from past four days	Mean from similar past days	Accuracy: 85%
Hossen et al. (2018)	UMass Smart Home Data Set	1 min	1 (hour)	weather	no	-	FFNN ⁴	MAPE ⁵ fridge: 5.24%
Singh and Yassine (2018)	UK-DALE	30 min	1 (hour/day)	appliances, on/off states, date-time	no	SVM ² , MLP ⁶	Bayesian network	Day Accuracy: 75.88%
Ji et al. (2020)	Pecan Street Data	1 min	60 (min)	operating states, temperature, hour	yes	hidden semi-Markov model (HSMM)	conditional HSMM	Fridge nRMSE ⁷ : 0.17
Jin et al. (2020)	not specified	1 min	1 (day)	on/off states, duration	-	Markov chain model	inhomogeneous Markov model	-
Razghandi and Turgut (2020a)	DRED	10 min	1 (10 min)	Last_seen_on/off, date, time	yes	RF ⁸ , FFNN ⁴	LSTM ⁹	Fridge nRMSE ⁷ : 0.076
Laouali I H (2021)	UK-DALE	6 sec	1 (6 sec)	-	no	LSTM ⁹ , AE ¹⁰ , CO ¹¹ , FHMM ¹² , Seq2Point ¹³	MLP ⁶	Fridge RMSE ¹⁴ /MAE ¹⁵ : 24.92/1.63
Razghandi et al. (2021b)	iHomeLab RAPT	10 min	6 (10 min)	weekday	yes	Vector ARMA ³ , SVR ¹⁶ , LSTM ⁹	Seq2Seq ¹⁷	Dryer RMSE ¹⁴ /nRMSE ⁷ /wMAPE ¹⁸ : 53.50/0.064/1.058
Razghandi et al. (2021a)	GREEND ^A	10 min	6 (10 min)	weekday	yes	Vector ARMA ³ , CNN ¹⁹ , LSTM ⁹	Seq2Seq ¹⁷	Fridge RMSE ¹⁴ /nRMSE ⁷ /MAE ¹⁵ : 43.782/0.174/2.134

^Abuilding 0, ¹k-Nearest Neighbour, ²support vector regression, ³autoregressive moving average, ⁴feed forward neural network, ⁵mean absolute percentage error, ⁶multilayer perceptron, ⁷normalized root mean squared error, ⁸random forest, ⁹long-short term memory, ¹⁰Autoencoder, ¹¹combinatorial optimisation, ¹²factorial hidden Markov model, ¹³Sequence-to-point, ¹⁴root mean squared error, ¹⁵mean absolute error, ¹⁶support vector regression, ¹⁷sequence-to-sequence, ¹⁸weighted mean absolute percentage error, ¹⁹convolutional neural network

lag of time. In the context of user-centered applications, long adaption periods of models and predictions discourage utilization and satisfaction.

To overcome this problem, direct approaches use time series forecasting methods to obtain the next load value from the most recent lagged time steps. In this field, research focuses on neural networks as a promising alternative capable of learning complex, nonlinear relationships between appliances and their environment. In single-step forecasting studied models include a nonlinear auto-regressive neural network predicting the next six-second time interval [Laouali et al., 2022] and a linearly activated multilayer perceptron (linear regression) forecasting daily consumption [Hossen et al., 2018] including weather features.

Reverting to machine learning solutions applied to appliance load forecasting Lachut et al. [2014] focus on the predictability of appliance loads and compares prediction accuracies across models for single-step time horizons from one hour up to one week ahead. The authors include date-time features and achieve accuracies up to 89% for hourly and 74% for daily predictions. Results on predictability across different homes show large variations.

Razghandi and Turgut [2020a] extend the univariate single time step approach and formulate a multivariate prediction problem by estimating load values of multiple appliances simultaneously. They design a long short-term memory network (LSTM) to predict the load values of multiple appliances for one time step ahead, comparing performances against a feed forward neural network (FFNN) and a random forest model. They additionally introduce *Last_seen_on* and *Last_seen_off* states as generated input features to reduce the overall errors. This multivariate prediction approach successfully captures dependencies between multiple output values of different appliances. This is an advantage over fitting separate algorithms for each output step.

In contrast and the most similar approach to the one proposed in this work, the same authors propose a framework to predict multiple future consumption values of single appliances, conditioning the model to learn dependencies among multiple time steps. Razghandi et al. [2021a] and Razghandi et al. [2021b] utilize an encoder-decoder type network called sequence-to-sequence model. The first variation uses long-short term memory layers, while the latter relies on bidirectional long-short term memory layers to predict load one hour ahead in 10 minute time steps.

The overview presented and outlined in Table 2.1 concludes the following: Firstly, non-deep learning approaches heavily rely on including important features for predictions while deep learning methods so far fail to utilize this additional potential. Secondly, reported deep learning approaches are limited to data granularity either smaller than 15 minutes or as aggregated as daily load values, with max forecasting horizons of six time steps resembling one hour. Assuming that individuals plan their day at least the day before and only once, practical models need larger prediction horizons covered with a more informative granularity of load estimates. Finally and regarding real-world applications, no study considers more than one data source for an equal set of appliances.

3 Methodology

This section describes a three-step framework to assess predictability, the engineered features and the deep learning architectures to forecast 24 load values. The predictability analysis forms expectations of model performance and quantifies the performance of feature groups and forecasting algorithms. The feature engineering step generates and groups similar features to distinguish the contribution of the data sources to predictions. The term features refers to variables containing either supplementary information or a reformulation of existing data (engineered features). The impact of different types of features is assessed and compared across four different datasets. The main step compares performances among different deep learning architectures and with non-deep learning (benchmark) algorithms. The following subsections introduce the methods used in this study.

3.1 Predictability

Predictability quantifies inherent information contained in a time series and assists in evaluating the predictive power of different forecasting methods. Model performance measures the probability of success yet it cannot provide an understanding for whether predictions improve. Intuitively, predictability estimates the highest level of performance possible for a time series and specifies whether the system is unpredictable or the model choice is poor.

A well-established measure of complexity in time series data is the permutation entropy (PE) proposed by Bandt and Pompe [2002]. PE captures the order relations between values and extracts a probability distribution of the ordinal patterns. Aquino et al. [2017] applies this PE to electric appliance loads mapping load histograms onto a Causality Complexity-Entropy Plane to contextualize electric load behavior.² This work relies on a modified version of the PE the weighted permutation entropy (wPE) measure formulated by Fadlallah et al. [2013]. wPE incorporates amplitude information to improve handling abrupt signal changes and more accurately assessing regular as well as noisy and (linearly) distorted data segments. The wPE is applicable to regular, chaotic, noisy or real-world time series and fit the volatile appliance load data better than the regular PE. wPE uses weighted relative frequencies defined by equation 3.1 to incorporate the amplitude information into the Shannon entropy formula 3.2.

$$p_w(\pi_i^{m,\tau}) = \frac{\sum_{j \leq N} 1_{u:\text{type}(u)=\pi_i}(X_j^{m,\tau}) * w_j}{\sum_{j \leq N} 1_{u:\text{type}(u) \in \Pi}(X_j^{m,\tau}) * w_j} \quad (3.1)$$

$$H_w(m, \tau) = - \sum_{i: \pi_i^{m,\tau} \in \Pi} p_w(\pi_i^{m,\tau}) \ln p_w(\pi_i^{m,\tau}) \quad (3.2)$$

The choice of weight values w_j reflects a specific feature or a combination of multiple features from each vector $X_j^{m,\tau}$. Following Fadlallah et al. [2013] the weights are computed by the variance of each neighbors vector of $X_j^{m,\tau}$ in equation 3.3 with $\bar{X}_j^{m,\tau}$ denoting its mean (equation 3.4).

$$w_j = \frac{1}{m} \sum_{k=1}^m m(x_{j+(k-1)\tau} - \bar{X}_j^{m,\tau})^2 \quad (3.3)$$

with

$$\bar{X}_j^{m,\tau} = \frac{1}{m} \sum_{k=1}^m m(x_{j+(k+1)\tau}) \quad (3.4)$$

The work in Riedl et al. [2013] gives a guideline on how to choose parameters optimally. The final parameter sets are reported in Appendix A.1.

3.2 Feature Engineering

The inclusion of features and their contribution to prediction accuracy within deep learning is hardly studied in the context of appliance level load modeling. Some approaches include numerical or one-hot encoded time features without reporting their influence on predictions. Research in other areas vastly confirms large benefits from including additional information, especially in deep learning. Presumably, additional features likewise improve forecasters in the appliance load domain. The following subsections describe included feature groups proven informative in the literature on aggregated household energy consumption. In total 10 feature groups are defined: date-time, weather, appliance, last seen on and last seen off (ls-on/ls-off), auto-regressive, interaction, automated auto-regressive feature

² The work in [Aquino et al., 2017] uses the REDD data.

engineering package (VEST) and phase space features as well as the aggregate feature group "weather and date-time features (w+dt)" and "all" (including all features).

3.2.1 Date-Time Features

Opinions and practices on whether and how to include date-time features vary substantially. Common variations in load forecasting include one-hot encoded, numerical encoded and sine cosine transformed time features [Candanedo et al., 2017], [Khatoon et al., 2014], [Hernandez et al., 2013]. Some, amongst others Razghandi et al. [2021a], argue against explicitly including date-time features in LSTM modeling as the positioning of the values within the input sequence already carries the time point information. Consequently, they exclusively include a numerical representation of weekday features, but no feature with the hour and minute of the day. Though sequentially ordered input structures of LSTM layers and numerically encoded time inputs fail to represent the cyclical nature of most date-time variables. A cyclical representation takes into account that the end and beginning of a sequence are numerically as close as time values in between, i.e. 23rd hour of the day is as close to hour zero as hour one to hour two [Ramezani et al., 2005].

In other domains of energy forecasting, such as forecasting load at electric charging sites [Unterluggauer et al., 2021] or forecasting power grid states [He et al., 2020], date-time features transformed with the sine and cosine function successfully improve prediction outcomes. Following listed examples, the hour of the day, the day of the week, the week of the month and, whenever more than a year of data is available, the month will each be represented by sine and cosine transformed values calculated as in equation 3.5. Further, the date-time feature group includes binary workday, holiday and weekend indicators [Sehovac and Grolinger, 2020a], [Bouktif et al., 2018].

$$\text{Sin}_{fe} = \sin(2\pi * n) \quad \text{and} \quad \text{Cos}_{fe} = \cos(2\pi * n) \quad (3.5)$$

with,

$$n = \begin{cases} \text{hour}/24 & fe = \text{hour} \\ \text{weekday}/7 & fe = \text{day of week} \\ \text{monthweek}/5 & fe = \text{week of month} \\ \text{month}/12 & fe = \text{month and traindata} > 1 \text{ year} \end{cases} \quad (3.6)$$

3.2.2 Weather Features

Weather features have been frequently proven to improve (non-deep learning) load predictors for appliance and aggregated electricity consumption of households [Sinimaa et al., 2021], [Gao et al., 2018] and [Hossen et al., 2018]. Weather is expected to influence appliance use as humans differ their behavior accordingly and some appliance electric consumption directly depend on environmental conditions such as temperature f.e. fridge or air conditioners. External factors influence the dependencies between load consumption and weather variables, i.e. thermostats. To assess the impact of weather features and their potential contribution to accurately predict energy usage this study includes the most commonly used weather features temperature, humidity and wind speed [Spichakova et al., 2019], [Mughees et al., 2021a].

3.2.3 Appliance Loads Features

Especially non-deep learning approaches concentrate on the dependencies between appliances and their potential to predict single appliance load profiles. Singh and Yassine [2018] find specific appliance combinations to occur often. Intuitively specific appliances tend to be used in combination such as washing machines and dryers. However, with longer prediction horizons load values of accompanying appliances precede with a time lag, i.e. information from the washing machine one hour ago is not available for the prediction of a dryers activity. Therefore, the predictive power of other appliance loads when modeling a specific load profile 24 hours ahead must be assessed carefully. This study integrates the load measures of selected appliances and defines their influence on a forecaster's performance.

3.2.4 Engineered Features

Auto-regressive features [Li et al., 2021] and statistical summary features such as mean and median [Smith et al., 2020] as well as average and standard deviation of load consumption over k-time steps [Wahab et al., 2021] positively impact aggregated load forecasting quality. Features especially summarizing a larger past time window might especially help predict appliances used less frequently than on a daily basis. Therefore the moving average and moving max value of the past 12, 24, 36 and 72 hours compose the auto-regressive feature group. Further, four simple interaction variables between each appliance pair (sum, product, mean and standard deviation) as well as the mean and standard deviation across all appliance loads form the interaction feature group to capture more complex dependencies among appliances.

Cerqueira et al. [2020] develop an automatic feature engineering package called VEST to build auto-regressive and summary features from time series data, which covers a more extensive set of engineered features. To profit from this research and available feature engineering packages, the study uses a feature set selected by the VEST feature engineering package for time series analysis in the VEST feature group. Equally, the study includes ls-on/ls-off states for the target appliance as proposed in [Razghandi and Turgut, 2020b]. This ls-on/ls-off feature group useful in a multivariate prediction setting might similarly contribute to performances in a multistep prediction setting.

3.2.5 Phase Space Reconstruction Features

Drezga and Rahman [1998] initially used features containing reconstructed dynamics of a chaotic system as an embedding method for load forecasting. These features require phase space reconstruction³ techniques utilized for aggregated load predictions [Zhang et al., 2008], [Fan et al., 2018] and [Shi et al., 2019]. Several undefined exogenous factors influence the electric use of appliances directly such as human activities or environmental conditions and indirectly via factors steering human behavior. As a consequence appliance load data shows complex characteristics such as multidimensional nonlinearity and high grades of uncertainty typical for dynamic systems [Fan et al., 2018]. Therefore, the motivation to transfer phase space reconstruction techniques to appliance load prediction assumes that the new phase space features reconstruct the more complex dynamics of a target appliance’s usage and represent immeasurable influences on load usage profiles.

Phase space reconstruction maps the observed time series into an embedding space that preserves the structure (topology) of the underlying dynamical system. To construct phase space reconstruction features, the target values are embedded in the space of their temporal lags using the Taken embedding [Takens, 1981].⁴ Appendix A.1 specifies software and parameters for the construction of the phase space features.

3.3 Prediction Algorithms

A vast selection of (hybrid) neural network architectures has proven to accurately predict multistep or multivariate sequential data. Subsequent subsections describe the deep learning architectures including LSTM, bidirectional long short-term memory network (BiLSTM), encoder-decoder networks, FFNN and CNN-LSTM.

3.3.1 Long-Short Term Memory Network

LSTM networks, initially proposed by Hochreiter and Schmidhuber [1997], are a type of recurrent neural network often used in time series prediction. They remember information from several past input steps while sequentially calculating outputs capturing the time dependencies of input variables. The architectural unique characteristics of LSTM Networks are the LSTM cell memory states that convey information across a chain of LSTM cell states and update new information only if considered important. LSTM cells process their own previous cell output h_{t-1} together with new input values x_t at time t and update cell memory states $C_{t-1} \rightarrow C_t$ to calculate the new output value h_t . In this process previous cell outputs h_{t-1} are filtered through input gates i_t , forget gates f_t , update gates \tilde{C}_t (g_t) and output gates o_t to find the important information for updating cell memory state and calculating cell outputs. The stepwise calculations of LSTM cell states are as follows:

$$f_t = \sigma_{f_t}(W_f \cdot [h_{t-1}, x_t] + b_f). \quad (3.7)$$

$$i_t = \sigma_{i_t}(W_i \cdot [h_{t-1}, x_t] + b_i). \quad (3.8)$$

$$\tilde{C}_t = \tanh(W_C \cdot [h_{t-1}, x_t] + b_C). \quad (3.9)$$

$$C_t = f_t \cdot C_{t-1} + i_t \cdot \tilde{C}_t. \quad (3.10)$$

$$o_t = \sigma_{o_t}(W_o \cdot [h_{t-1}, x_t] + b_o). \quad (3.11)$$

$$h_t = o_t * \tanh(C_t). \quad (3.12)$$

As demonstrated in Figure 3.1, first the input and the previous cell output are pushed through the sigmoid forget layer 3.7 which determines what information from the previous cell state to keep or not to keep. Secondly, the sigmoid

³ Phase space reconstruction is the foundation of nonlinear time series analysis describing the reconstruction of complete system dynamics using a single time series [Ali Shah et al., 2019] from [Bradley and Kantz, 2015]. ⁴ Takens’ theorem, also named the delay embedding theorem, shows that a time series of measurements of a single observable can be used to reconstruct qualitative features of the underlying phase space system [Huke, 2006]. A phase space formulates the space in which all possible states of a system are represented. In this application, a phase space representation of the target appliance loads describes all possible target values and their complex relation to each other.

Figure 3.1:
Functionality of the LSTM-Unit (Image Source: Olah [2015a])

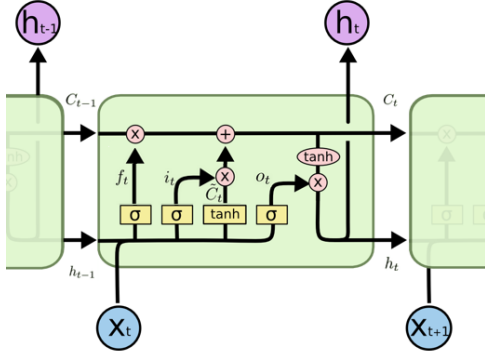
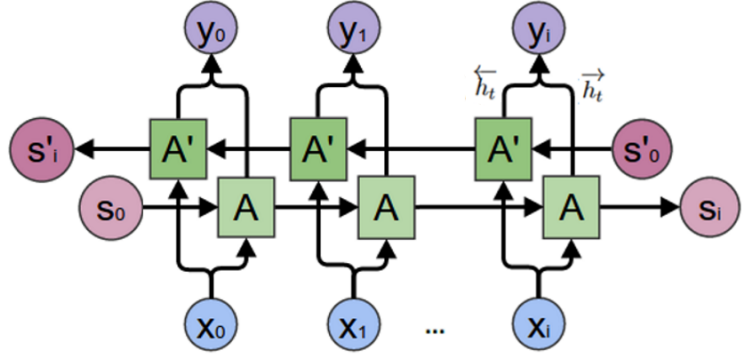


Figure 3.2:
Functionality of the BiLSTM-Layer (Image Source: Olah [2015b])



input layer 3.8 decides which values of the cell state to update and the tanh update layer 3.9 calculates candidate values for updating cell states. Equation 3.10 calculates the updated cell states. Another layer, the sigmoid output layer 3.11, decides which parts of the cell state to output. The updated cell states are then pushed through a \tanh layer and multiplied by the output filter in Equation 3.12. This cell output together with new input values initiates the next update process of the cell state and repeats itself iteratively. This structure remembers long-term dependencies and due to the multiple gate calculations form an additive structure of the gradient term. The gradient term updates layer weights by calculating derivatives in the backward propagation process. In this context, an additive structure of the gradient term reduces the likelihood of exploding and vanishing gradients, which leads to a more stable network training making LSTM networks a reliable choice for time series predictions [Hochreiter and Schmidhuber, 1997].

3.3.2 Bidirectional Long-Short Term Memory Network

LSTM layers forward pass input values sequentially. Consequently the first output of an LSTM cell is based solely on the first input and fails to use all values within the input sequence. A BiLSTM, proposed by Graves et al. [2005], enables all LSTM cell states to use information from the complete input sequence, passing it forward and backward through the network (Figure 3.2). To add a backward pass the BiLSTM adapts the standard LSTM network by adding a separated hidden layer processing sequences in reverse. The forward layer processes the input sequence from beginning to end the backward hidden layer from end to beginning. Every BiLSTM layer contains double the number of memory cells. The information of the forward and backward pass is stored in separate hidden states (\vec{h}_t and \overleftarrow{h}_t) which are concatenated to produce the final hidden state h_t . At any time step t , the forward and backward layer outputs of a BiLSTM cell are computed using the standard LSTM unit's operating equations 3.7–3.11. Then the final hidden state vector is computed by combining the hidden state sequences in 3.13:

$$y_t = \oplus(\vec{h}_t, \overleftarrow{h}_t). \quad (3.13)$$

where \oplus is a concatenate function. It should be noted that other operations, such as summation, multiplication, or averages, can be used instead. BiLSTM Networks initially improved long-range context processing in Natural Language Processing [Graves et al., 2005]. Momentarily, they frequently deliver state of the art performance in (load) time series predictions [Mughees et al., 2021b] and outperform deep learning architectures such as the LSTM and convolutional neural network (CNN) [Fadlallah et al., 2013].

3.3.3 Encoder-Decoder Networks

Encoder-decoder models, such as the sequence-to-sequence model, likewise originate from language translation [Sutskever et al., 2014] and prove powerful in time series forecasting [Du et al., 2018], [Sehovac and Grolinger, 2020b] and [Fadlallah et al., 2013]. An encoder-decoder architecture comprises two network parts, an encoder network and a decoder network. The encoder calculates a hidden representation of the inputs encoded in hidden states and passes them on to the decoder network for calculating predictions. The difference to standard neural network training is the transfer of states instead of layer outputs between the encoder and decoder and often the two parts are

Figure 3.3:
S2S-Model with Reversed Sequence Decoder (Image Source: Razghandi et al. [2021b])

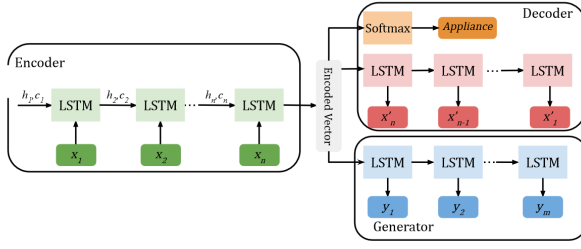
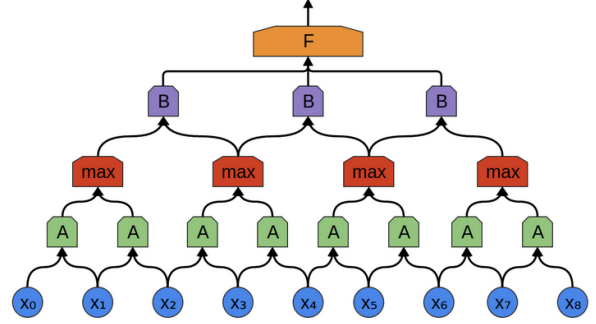


Figure 3.4:
Functionality of 1D-CNN-Layer (Image Source: Olah [2015a])



pre-trained separately before the final prediction stage. This study includes two variations of the sequence-to-sequence network. The sequence-to-sequence model used by Razghandi et al. [2021b] further called S2S reversed and a variation of the sequence-to-sequence model proposed in the winning solution to the web traffic time series forecasting challenge introduced by Angioi [2020] called sequence-to-sequence with an encoder learning a context embedding (S2S context).

The S2S reversed uses two decoders shown in Figure ?? . In the first step the encoder trains together with a decoder that learns the reversed representation of the input sequence. This forces the encoder to include a backward representation of the input window in its hidden states. In a second training step, the weights of the pre-trained encoder initialize the training of the second decoder, which learns to predict the next output sequence. As shown in section 5 the training time is prolonged substantially by this double decoder network setup.

The second variation S2S context uses no pre-training, instead, input information is separated into past observations of the target sequence and additional features. The encoder calculates a hidden state representation of the additional features as a sort of context. Transferring these states initializes the decoder network. The decoder uses the past target sequence as input together with the encoder weights to predict the next output sequence. This variation trains only one network and reduces computation times compared to S2S reversed. Both networks use standard LSTM-layers within the encoder and decoder parts.

3.3.4 Feed Forward Neural Network

The simplest deep learning architecture is the feed forward neural network, where information flows only in one direction (forward). The network consists of multiple layers where each node is connected to all the following nodes in the next layer. The simple structure gives this type of network an advantage in computational speed. However, its simplicity potentially results in a less complex representation of dependencies among variables reducing performance. In detail a feed forward network defines a mapping of inputs x on outputs y in the form of $y = f(x; \theta)$. It learns the value of the parameters θ that result in the best function approximation f of y . In FFNN there are no feedback connections as in recurrent neural networks like LSTMs [Goodfellow et al., 2016].

3.3.5 Convolutional Long-Short Term Memory Network

Another deep learning architecture proposed for time series prediction is the CNN. Originally used for image processing by LeCun et al. [1989] this architecture uses convolutional layers consisting of kernel matrices that convolve the time series information in each layer and thereby extract more complex features. This process has proven to extract important features, especially in multivariate prediction problems such as load forecasting [Amarasinghe et al., 2017].

Figure ?? depicts the architecture of the CNN-layer. Typically, time series problems use 1D convolutions. They mimic moving average computations and extract features across time steps and time series (spacial hierarchies). When using a 1D convolutional layer, a one-dimensional kernel with size k functions like a weight mask that multiplied with the input layer fold inputs together to form the layer output. Often the convolutional layer output is passed on through an activation function leaky rectified linear unit (LeakyReLU) and through a pooling layer. The pooling layer (i.e. max pooling) summarizes the feature map into a lower-dimensional representation, also called smoothing, thereby reducing the influence of small data fluctuations. The final output is flattened to either produce predictions or to be passed on to a fully connected layer. As proven by Yan et al. [2018] the predictions benefit from adding a final LSTM layer to predict final sequential output windows forming a CNN-LSTM model.

3.4 Benchmark Models

Two prediction algorithms, one tree-based and one based on support vector regression (SVR) benchmark the deep learning performances. eXtreme Gradient Boosting (XGBoost) is a widely used and stable performing machine learning method while the MSVR is a multioutput adaption of the SVR. The single SVR frequently serves as a well-performing benchmark in single output time series problems.

3.4.1 XGBoost

XGBoost first proposed by Chen and Guestrin [2016] is a classic tree-based algorithm using a gradient boosting framework. The intuition behind boosting is adding new decision trees predicting the values better where the initial model failed to give good results. Adding a multiple of these boosting trees to an ensemble of trees is expected to improve predictions by a multiple. There is no ready implemented version for multistep regression problems using the XGBoost algorithm. This implies that one model for each time step must be fitted.

3.4.2 Multiple-Output Support Vector Regression

Even though benchmarking often uses SVR, in multistep prediction problems the basic SVR structure restricts the algorithm to singular output values. This requires either to use predicted values iteratively as input to get the next prediction step or to fit one SVR for each output step. In their work Bao et al. [2014] further develop the initial version of the MSVR first proposed by Pérez-Cruz et al. [2002] and design a SVR for multistep time series prediction problems. Bao et al. [2014] prove the MSVR to outperform the iterative and multi-model SVR approach in multistep time series prediction while keeping computational costs low. The MSVR preserves the stochastic dependencies within the time series data by estimating a multidimensional output. This facilitates mapping the underlying time series dynamics by estimating a multidimensional output [Pérez-Cruz et al., 2002]. For the full derivation of the MSVR solution see Bao et al. [2014]. Pre-tests of all three prediction strategies on the REFIT electrical load measurements dataset (REFIT) data in this study confirms the effectiveness and superior performance of the MSVR over the direct and iterative standard SVR replicating results in Bao et al. [2014].

4 Data and Experimental Design

All models are fitted to data from four homes, taken from datasets covering different geographic locations in Europe and North America. Table 4.1 summarizes details on the datasets and indicates whether the homes use a thermostat. The Almanac of Minutely Power dataset Version 2 (AMPds2) [Makonin et al., 2016] is the largest dataset covering two full years of data. The REFIT [Murray et al., 2017] spans a period of almost two years but contains a wider gap of six weeks of missing data. GREEND Electrical ENergy Dataset (GREEND) [Monacchi et al., 2014] and Pecan Street Data (PecanSD) Parson et al. [2015] are smaller datasets with data from 10 months and six months respectively with the most recent data reported from 2019 in Pecan Street. If available, the study uses the weather features published alongside the datasets. Otherwise, the preprocessing step merged historic weather data from a local weather station⁵. The distance to the nearest weather stations is maximum 10 kilometers and the main pool of appliances selected contains appliances responsible for a large part of total appliance electric usages such as fridge, washing machine, dryer, dishwasher and television.

Table 4.1: Datasets

Dataset	Country	Years	WS Dist.	Appliances	Thermostat	Train/Validation/Test
REFIT*	UK, Leicester	2013-11-04/2015-05-09	3 km	fridge, dryer, washing machine, dishwasher, television	no	7,540/1,884/2,807
AMPds2	Canada, British Columbia	2012-04-01/2014-03-31	< 1 km	fridge, dryer, washing machine, dishwasher, television	yes	11,710/2,927/2,883
GREEND*	Austria, Kärnten	2013-12-07/2014-10-13	< 10 km**	fridge, washing machine, dishwasher, television	n.a.	4,116/1,029/600
PecanSD*	USA, New York	2019-05-01/2019-10-31	< 5 km**	fridge, dryer, washing machine, dishwasher	n.a.	2,353/588/1,447

* Selected houses: GREEND - building 0; Pecan Street - house ID 3996; REFIT - house 1;

** historic weather data from a nearby weather station

⁵ obtained from <https://openweathermap.org/>

4.1 Preprocessing

The first step aggregates all original load measurements to hourly measurements and split into train, test and validation sets. Table 4.1 describes training, validation and test split sizes. Test data sizes vary due to testing periods starting at the beginning of a month but roughly lie between 20% and 10% of the full data set size. In all cases, training algorithms use 20% of training data samples for validation.

The preprocessing pipeline imputes missing date-time values, not exceeding a gap larger than three days. The mean of the same hour on the same weekday at previous time steps imputes the missing load values to maintain presumably regular consumption patterns for weekdays. Weather variables use the mean of the corresponding week to impute values resembling values close to the same point in time. For longer time gaps this method preserves the data structure, as opposed to, i.e. forward filling introducing significantly different data patterns. The wide data gap in the REFIT dataset was kept unimputed.

To detect outliers, the 90% winsorization calculates the 5th and 95th percentiles of the data and deletes all values below and above the lower and upper bounds. The subsequent step imputes the deleted measures by forward filling the previous value. In this case, forward imputation has only minor effects on the data structure and is a highly efficient method. Only fridge usage profiles in REFIT and PecanSD justified using outlier replacements in seven and three cases respectively. Similarly, among weather variables only wind speed in REFIT contained extreme values. A check on historic wind speed data for reported date and location additionally verified the identified values as outliers.

Further, the StandardScaler function from sklearn standardizes features by removing the mean and scaling to unit variance with the formula $z = (x - u)/s$. Standardization of data identifies the output range beforehand and reduces the impact of larger numbers to stabilize the training process. Note that to normalize training values only the first 80% of observations within the time series data were used to fit the StandardScaler to avoid information overspill.

After computing the features on the imputed and normalized data, rolling windows select input and output windows with 24 values (hours) comprising the training dataset. In a rolling window approach, the next data sample shifts by one value. For testing data, the experiment uses a slicing windows approach, which copies the real-world scenario where the next new 24 observations are presented all at once, not each hour. Hence the next data sample is the former sample shifted by 24 time values. Validation sets are constructed from the training set after the full preprocessing procedure.

4.2 Model Setup

Model input shapes after data preparation are (N, ts, f) with N equal to the number of samples, ts the number of time steps (24) and f the number of features. XGBoost, MSVR and FFNN require a flattened input shape, where the feature and time step dimension is flattened out to take the form $(N, ts \cdot f)$. To fit input into the CNN-LSTM model original inputs are extended to a fourth dimension to $(N, ts, f, 1)$ to satisfy CNN input requirements. Most of the feature groups fit well into this shape. However, selected VEST features and phase space transformations of the target variable change shapes to $(70, 1)$ and $(23, 2)$ respectively. As these transformations break up the sequential character of the input data the seq2seq architectures and the MSVR are not considered when looking at the impact of VEST and phase space features. The adaptations of the architecture needed to extract correct output from the adapted input dimensions make the models incomparable.

Model architectures use the TensorFlow framework with GPU support for tuning and training. For detailed parameter settings and tuning spaces see Table ?? in Appendix A.2. All models were trained using a Google Colab Pro account with priority access to high-memory virtual machines (32 GB RAM) and GPU (T4 or P100 GPU) support. Unfortunately, as Colab resources are distributed among users, training times might vary on equal training tasks depending on the computing capacity provided.

4.3 Evaluation Metrics

Mainly the root mean squared error (RMSE), normalized root mean squared error (nRMSE) and a 95 percent accuracy score (acc95) evaluate the presented results. The RMSE measures the average magnitude of prediction errors calculated with a quadratic scoring rule that penalizes larger results more and is defined in 4.2. The nRMSE is a scale-independent metric used by other comparable studies. It relates the RMSE to the observed value range by the Formula in 4.1.

The accuracy at the 95% level acc95 (see equation 4.3) calculates the sum of all predictions deviating less than 5% from the true value and reports the share of non-deviating values in percent off all values. Lachut et al. [2014] also report the acc95 as an indicator for predictability. The acc95 serves as a proxy to report the number of correctly

predicted values and sets the performance indicated by the RMSE and the nRMSE into relation. Additionally and to ensure comparability to related literature, the results on GREEND report the mean absolute error (MAE). The MAE is defined in 4.4 and measures the average magnitude of prediction errors.

$$nRMSE = \frac{nRMSE}{\max_{y_j} - \min_{y_j}}. \quad (4.1)$$

$$RMSE = \sqrt{\left(\frac{1}{n}\right) \sum_{i=1}^n (y_j - \hat{y}_j)^2}. \quad (4.2)$$

$$acc95 = \begin{cases} 0 & \frac{|\hat{y}_j| - |y_j| * 100}{|y_j|} > 5 \\ 1 & \frac{|\hat{y}_j| - |y_j| * 100}{|y_j|} \leq 5 \end{cases} \quad (4.3)$$

$$MAE = \frac{1}{n} \sum_{i=1}^n |y_j - \hat{y}_j|. \quad (4.4)$$

Additionally, the mean absolute scaled error (MASE) defined by equation 4.5 reports the effectiveness of the forecasting algorithm with respect to a seasonal naïve forecaster [Hyndman and Koehler, 2006]. A MASE lower than one indicates better performance, f.e. a MASE of 0.5 implies that a model would have double the predictive power of a naïve forecaster. In the case of a large percentage of zero values in the data, the MASE more reliably measures the predictive capacity of models than the combination of the nRMSE and the acc95.

$$MASE = \frac{MAE}{MAE_{naive}} = \frac{MAE}{\frac{1}{n} \sum_{i=1}^n |y_j - x_j|} \quad (4.5)$$

5 Results

This chapter groups results in three parts. The first two subsections report on data predictability and important features. The third section elaborates on the highest performing models, prediction stability across datasets, reliable model-feature combinations and suitability of CNN-LSTM and S2S context models for the task at hand. All subsections will first focus on results for the fridge appliance across all data sources and second compare these results to performances on other appliance types. For appliance types except for fridge the presented results include only outcomes of REFIT. Additionally, Table ?? and Figures 5.4 and 5.5 compare training duration across models to verify the applicability of presented approaches for customer-oriented solutions.

5.1 Predictability

The wPE measures a considerable amount of noise in the reported appliance load data similar to results in the related literature [Aquino et al., 2017]. Further, data predictabilities of fridge profiles show higher accuracies on REFIT in comparison to Lachut et al. [2014] who reports accuracies between 50% and 74% a day ahead. The combination of these findings validates the wPE as an effective indicator for predictability and verifies the effectiveness of proposed models over simpler statistical approaches in Lachut et al. [2014]. The wPE approach is suitable to pre-assess potential of prediction modeling and the amount of predictable data.

Overall the wPE reliably assesses, which appliances and datasets are easier to predict. Models reach higher accuracies on prediction tasks specified as easier to predict and lower otherwise. Entropy values above 0.5 indicate a significant amount of randomness in the data [Bandt and Pompe, 2002]. According to Figure 5.1 the dishwasher and the dryer as well as fridge profiles on REFIT show lower complexity compared to the fridge and the television and fridge profiles on the other datasets. The wPE analysis indicates larger divergence between the television and washing machine than measured accuracies confirm. This indicates that models better fit television profiles with a higher data complexity. Further in Table 5.1 the predictive power of models measured in terms of the MASE values is higher for GREEND and AMPds2 as well as for fridge and washing machine. In combination, both measures confirm that deep learning approaches perform stronger whenever data complexity is higher.

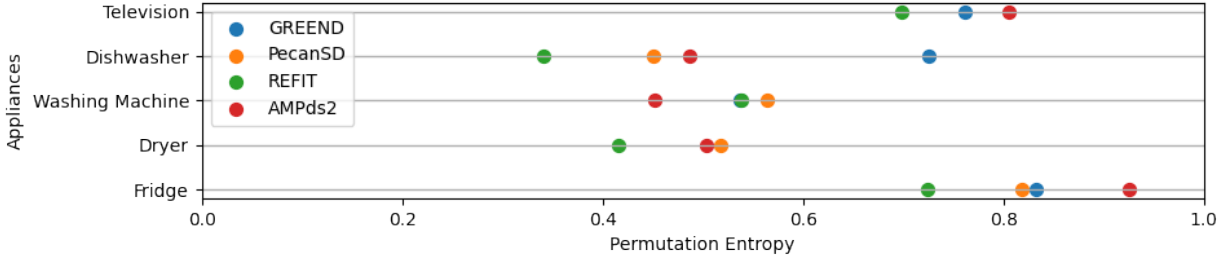
Figure 5.1:
Weighted Permutation Entropy for All Appliances and Datasets

Table 5.1: MASE Values Across Datasets

Data	Max	Min	Model Min	FE Min
GREENSD	0.9362	0.6792	LSTM	date-time
PecanSD	0.9656	0.7968	S2S context	weather and date-time
REFIT	0.8755	0.7927	CNN-LSTM	phase space
AMPds2	0.9208	0.7057	CNN-LSTM	date-time

5.2 Important Feature Groups

Figures 5.2 and 5.3 visualize the impact of features on predictions. It becomes clear that sine cosine encoded date-time features and the holiday indicator are the most important features, followed by weather features and ls-on/ls-off indicators. The impact of engineered features remains mixed across the datasets.

Date-time features positively impact prediction quality most frequently across all datasets and provide the largest improvements compared to other feature groups. Especially in combination with weather features, models highly profit from the cyclical information added to the sequential input improving prediction accuracy and error margins. This underlines the importance of including date-time features. Both numerical encoding of date-time features and one-hot encoded time features yielded worse results in comparison to predicting the target from its past values across all datasets.

The second most important features are weather indicators, despite their less consistent contribution across datasets. Weather features perform stronger in overall error on the nRMSE across datasets, while gains in acc95 depend on the underlying data with the risk of worsening the performance. For example, on the AMPds2 dataset performance drops significantly when including weather features. The household in the AMPds2 uses thermostats in each room. This most likely corrupts the potential information contained in outdoor environmental variables, when no thermostat is

Table 5.2: MASE Values Across Appliances on REFIT

Appliance	Max	Min	Model Min	FE Min
fridge	0.8755	0.7948	CNN-LSTM	weather
washing machine	1.5525	0.7595	LSTM	w + dt
television	1.3974	1.0758	LSTM	w + dt
dishwasher	2.0960	0.8204	LSTM	appliances
dryer	6.1995	1.2514	LSTM	appliances

Figure 5.2:
Changes in Mean nRMSE Scores per Feature Group

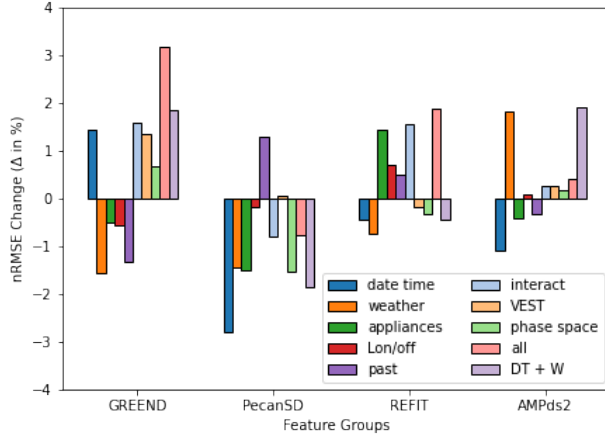
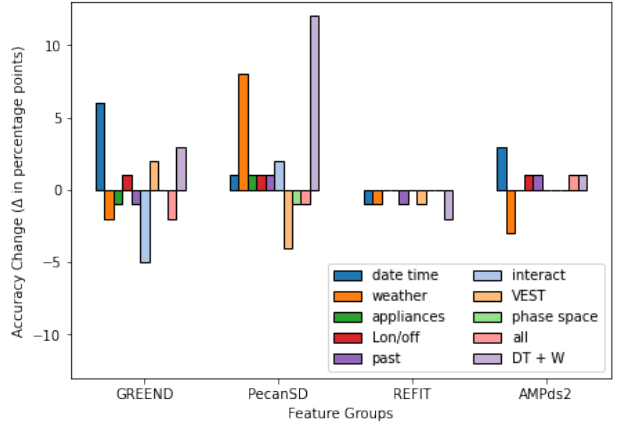


Figure 5.3:
Changes in Mean Accuracy per Feature Group



in place. Although weather features seem to be an influential factor for load predictions, their utility for predictive performance depends on other external factors, possibly not always available to application providers.

Phase space features mostly influence the overall error margin, without a clear tendency across models and datasets. However, looking closer at the results for individual model-feature combinations, interestingly, phase space features combined with CNN-LSTM model consistently show a small improvement of the nRMSE mostly without decreasing accuracy. This holds true across datasets and appliance types. The phase space reconstruction breaks up the sequential structure of the inputs complicating the sequential processing of values. Conclusively, the convolutional processing provides a better fit to the new data structure than sequential layer designs.

All other feature groups show small irregular effects across datasets. Their explanatory value for the target appliance loads depend on individual household properties and are not universal explanatory. Similarly, increasing performance through engineering past, summarizing and auto-correlated features, depends on the underlying data and requires a more in-depth feature selection on individual case basis.

5.3 Model Evaluation

According to Figure 5.4 and 5.5 nearly all deep learning models outperform the benchmarks in accuracy, except for REFIT where the XGBoost scores the highest. However, the high accuracy of the XGBoost approach evidently requires significant concessions to higher error scores, while deep learning alternatives reach comparably high accuracy with lower error scores. This proves the consistency of deep learning performance across data sources and their good fit to complex appliance profiles.

Comparing the best performing model-feature combinations referenced in Table ?? the LSTM delivers high and stable performances across all datasets when combined with varying feature combinations. The LSTM always ranks among the highest predictive performances. Especially for data with lower predictability, the LSTM heavily draws information from date-time features.

The S2S reversed shows a solid performance across feature groups on average. However, the S2S reversed is computationally expensive, resulting in longer training times This can be seen in Table 5.3. Comparatively, the less complex S2S context architecture outperforms the S2S reversed on most of the predictions while maintaining a faster runtime (3 min 52 seconds on average). Further results indicate that the S2S context seems to perform the best on television and AMPds2 hinting at a good fit on irregular data and appliance types. On the AMPds2, marked as the least predictable dataset, the S2S reversed reaches the highest performance in terms of accuracies (see Table ??).

The MSVR generally performs very strongly in terms of overall errors alongside LSTM and S2S reversed especially for appliances with many zero values. Less consistent results for the MSVR on the acc95 score show performance beneath deep learning alternatives. Lastly, the MSVR outperforms the XGBoost benchmark as well as the random forest algorithm⁶.

⁶ Results obtained with a random forest algorithm are not reported as exponentially growing prediction times disqualify it as a candidate for user-centric applications.

Figure 5.4:
Changes in Mean nRMSE Scores per Models

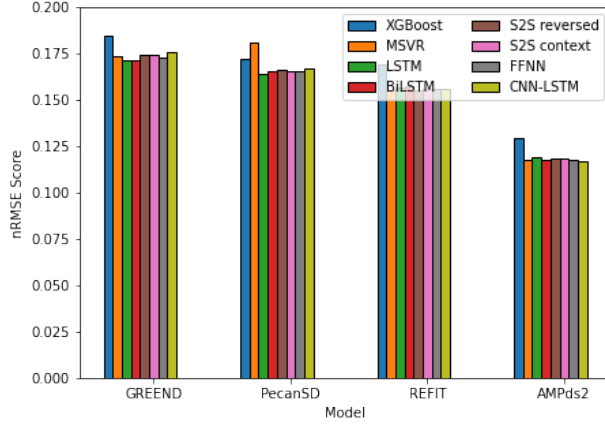


Figure 5.5:
Changes in Mean Accuracy per Models

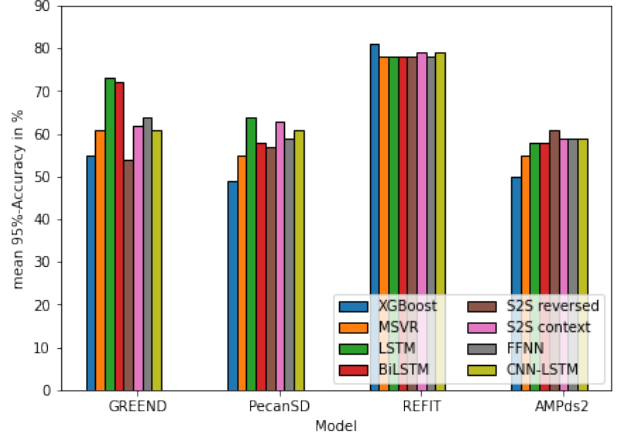


Table 5.3: Highest Performing Model and Feature Group Across Datasets

Highest Performing Model and Feature Groups					
Dataset	RMSE	nRMSE	Accuracy	Model	Feature Group
GREEND	21.3247	0.1710	0.5902	LSTM	weather
	22.8570	0.1833	0.7335	LSTM	date-time
PecanSD	22.0187	0.1612	0.3765	MSVR	date-time
	22.9568	0.1681	0.6416	LSTM	w+dt
REFIT	15.7191	0.1552	0.7768	MSVR	baseline
	17.7696	0.1755	0.8092	XGBoost	appliances
	15.9663	0.1577	0.7768	LSTM	interact
AMPds2	22.2304	0.1172	0.5873	CNN-LSTM	date-time
	22.5335	0.1188	0.6076	S2S reversed	weather
	22.5224	0.1187	0.5808	LSTM	date-time

Highest Performing Model and Feature Group for Each Appliance on REFIT

Dataset	RMSE	nRMSE	Accuracy	Model	Feature Group
dryer	18.0780	0.0378	1.0000	FFNN	appliances
dishwasher	98.8423	0.0976	0.9702	MSVR	date-time
washing machine	95.1288	0.0422	0.9397	MSVR	appliances
television	9.0308	0.2331	0.9275	MSVR	date-time
	9.5590	0.2467	0.9384	S2S context	appliances

5.3.1 Performance on Different Appliance Types

Results for other appliance types reported in Tables ?? and 5.2 confirm the significance of date-time and weather as well as appliance features. When evaluating performance on other appliances it is important to keep in mind the high percentage of zero values. These appliances stay turned off most of the time with zero value percentages in the training data above 63% for television and above 80% for the rest in comparison to the fridge with only 25% of zero values. High accuracies on these appliances are equally attainable by a predictor issuing zero all the time. In this case, reverting to the more reliant MASE metric in Table 5.2 consistently reports the LSTM to provide the highest predictive power among algorithms and across different appliance types. The results confirm the superiority of the LSTM model alongside weather, date-time and appliance features.

Interestingly, MASE values for television and dryer are higher than 1 indicating that models struggle to predict better than a naive forecaster. Especially for the dryer, this result contradicts the high predictability measured in the weighted permutation entropy. Interpreting these results, concludes that even though predictability of data is high, the models struggle to learn a proper representation, when a large share of the data contains equal values. For models to learn a representation regardless, either requires a larger ground truth database for training or specialized forecasting algorithms detecting anomalies.

5.3.2 Training Time

Deployment of user friendly applications requires fast and scalable algorithms. Training duration of an algorithm on differently sized feature sets approximates both performance indicators. Table 5.3 reports summarized training duration of presented model architectures across different sets of features. With the second shortest duration, the LSTM confirms its fitness as a practical solution. In general training times with deep learning (except CNN-LSTM) vary little among different feature groups confirming their scalability to higher feature dimensions. Using S2S reversed for production, requires higher engineering efforts for efficient computation or more powerful computation resources, as computation times are by far the highest.

Table 5.3: Training Time in Seconds

computation time	XGBoost	MSVR	LSTM	BiLSTM	S2S reversed	S2S context	FFNN	CNN-LSTM
mean	15	63	24	22	266	37	6	24
max	66	73	26	24	298	40	8	55
min	8	45	22	20	243	34	5	20

6 Discussion

This section embeds reported results into related work and discusses implications and importance of results for industry and the research community.

Razghandi and Turgut [2020a] demonstrate the case in which important features for multivariate appliance load prediction apply less strongly to multistep output. In their work, including ls-on/ls-off features largely improves the reported nRMSE of their LSTM network (ca. +80%). The results in this study show only a small positive impact across datasets. Importantly, the referenced authors use a different dataset⁷ and forecast one time step for multiple appliances. Naturally, the influence of the observed ls-on/ls-off states 24 hours ago are not as informative as the observation of the last hour.

The LSTM model proves itself as a strong alternative to the S2S reversed proposed for shorter prediction tasks in Table ?. On the same data, the presented LSTM model including weather features outperforms their model on all three metrics. Subsequently in both, performance and training duration, the simpler LSTM network is preferable over the S2S reversed. However, the comparison should be taken carefully, as models in Razghandi et al. [2021b] predict a 10-min resolution as opposed to one hour in this application. A more coarse forecasting granularity might be easier to predict.

The presented LSTM outperforms the Hidden Semi Markov Model of Ji et al. [2020] that predicts the next 60 time steps of one-minute data. The differences become more evident when considering the focus of Ji et al. [2020] on

⁷ The authors use the DRED dataset.

groups of similar appliances including up to 50 appliances in reported target values. In previous research, single appliance loads are associated with higher error margins. Conclusively, the presented models show competitive results to the statistical approach in Ji et al. [2020].

6.1 Contributions

Deep learning approaches for appliance level load prediction significantly improve with environmental and cyclical time-related information. Especially, the impact of sine cosine encoded features contradicts research assuming the sequential ordering of input values to suffice in LSTM feature modeling and adds to the debate on efficiently encoded time features. Less complex statistical summary features, like the auto-regressive and interaction features, show lower impact and confirm the high capacity of deep learning models to autonomously extract this information from feature sets. On the other hand, chosen architectures demonstrate difficulties extracting valuable information from highly complex features, such as phase space reconstruction variables. Most likely, breaking up the sequential character of inputs disrupts efficient information extraction by models that rely on this structure. Conclusively, sequential models are no good fit for phase space reconstruction features. Correlations presented in appliance features seem of reduced importance in a multistep single appliance prediction task.

Further, the results confirm that deep learning approach are superior to alternative time series prediction methods, particularly when dealing with irregular data structures. Simpler architectures such as the LSTM and the S2S context showed consistently higher performance over more complex design variations such as the BiLSTM or S2S reversed. In conclusion, higher architectural complexity based on similar single-layer designs have only limited potential to improve predictions. Nevertheless, the potential and flexibility of new deep learning techniques and their expected development support deep learning as a trustworthy approach for modeling single appliance load profiles.

MSVR outperforms tree-based alternatives frequently applied in related literature. This application therefore serves as a benchmark for future research work. Benchmarking with the MSVR challenges deep learning algorithms in terms of RMSE and nRMSE, especially on less variable data. With a consistently low nRMSE this model might even be a justified choice, whenever applications strongly rely on a lower error margin over higher accuracies. An example might be when high prediction errors are associated with high costs. In this case, outperforming the MSVR indicates a good model fit to the data.

Expectations of superior performance from the CNN-LSTM were not confirmed. Nevertheless, the model shows the best abilities to process highly complex non-sequential features such as the phase space indicators. This promising solution from aggregated load profiling specifically extracts information from input features well. Hence, the moderate performance ranking questions the importance of an additional feature extraction layer for the task at hand.

The newly applied architecture, S2S context, succeeds in outperforming its counterpart the S2S reversed, with significantly less computation time. Accuracy rates fluctuate less across feature groups and indicate a lower dependence of the encoder-decoder structure on the selection of input features. Conclusively, the sequence-to-sequence structure might be preferred whenever less capacity for detailed feature engineering and selection is available.

Overall and in comparison to the existing literature on appliance profiling, transferring the feature engineering from non-deep learning approaches to the more efficient deep learning method largely improves performances. Reevaluating existing deep learning approaches for the more practical task of forecasting 24 hourly load values, contradict the proven superiority of sequence-to-sequence modeling over simpler LSTM models in Razghandi et al. [2021b]. Seemingly, the advantage of reverse sequence modeling diminishes with a more coarse forecasting granularity. Instead, additional information from date-time and weather features become important.

6.2 Implications

The presented three step framework is directly deployable in industry applications. Incorporating the presented framework would enable home energy management systems (HEMS) and recommendation applications to transparently provide consumers with insights into their consumption profiles and showcase potential energy-savings. The predictability analysis actively manages expectations by pre-reporting expected error margins and the complexity of appliances loads chosen for predictions. The forecasting step enhanced by cyclical features and weather indicators improve the quality of existing applications and thereby comply with consumers' expectations. Further, adequately addressing consumers expectations increases satisfaction and participation, the key indicator of success in any energy-saving program [Sun and Hong, 2017].

Secondly, conducting a predictability analysis prior to deployment of a modeling framework effectively assesses data potential and pre-identifies correct model structures. This speeds up application engineering and saves costs for smart home application providers, ultimately reducing entry costs of new app providers to design solutions. Further, easily

accessible and low-cost engineering further nurtures innovation and development for applications tailored to consumers' needs motivating new consumers to engage in energy-saving behaviors.

6.3 Limitations

Selected deep learning architectures show restricted capacity to model all types of appliances usage profiles. Profiles of seldomly used appliances require modeling designs specialized in detecting the few positive states or larger data samples to correctly learn a profile's specificity. An interesting approach responding to a higher demand for information within these tasks extends the multistep approach by a multivariate dimension. Simultaneously modeling multiple appliance profiles in one model could ascertain whether dependencies among appliances and the prediction values of related devices provide the additional information needed to correctly predict seldom values.

The use of different geographical locations verifies the robustness of the presented results. However, the scope of this study is limited to the western hemisphere and leaves additional verification for other regions pending. Similarly, due to restrictions in available data highly promising influential features could not be tested. As an example, smart home applications might have local access to a family calendar through connected smartphone applications. The availability of this data limits a complete analysis of the predictive power of important features in appliance load modeling. Nevertheless, this work succeeds in guiding intuitions for the importance of not available features. Additionally, the predictability analysis provides fast testing for new data to form expectations for new appliance data sources.

6.4 Recommendations

In deployment, developers of smart home applications reliant on appliance load prediction would benefit from conducting a predictability analysis prior to implementation. This can guide suitable model choice and points to appliances requiring additional components capturing seldom behavior. A predictability step as conducted in the presented framework identifies data with a good fit to the model especially when the data structure is noisy and appliances are hardly used. In deployment this will save engineering costs and avoid promising model application performances that cannot be met.

secondly, implementation of smart meter systems and recommender applications should time label smart meter readings and connect the HEMS system to weather data either from the home itself or from a local weather station to enhance their system robustness. Accompanying options to specify household default characteristics, such as thermostat usage, delivers additional insights and prevents corrupted results from external influences. Generally advanced engineering and additional processing of input features is not needed. Rather efforts might go into more data collection of promising features not included in this study and described in the following section.

6.5 Future Work

Future research on multistep, multi-appliance profiling can address some of the limitations stated in Section 6.3. This task comprises a higher output complexity and requires high capacity deep learning architectures such as transformers. Interestingly, transformers process complete input sequences without relying on past hidden states and sequential processing. This could preserve the long-term dependencies within time-ordered sequences and capture the cyclical characteristics important within the presented topic. Equally, mechanisms such as multi-head attention and positional embedding designed to capture the multivariate dependencies might effectively predict different appliance usage profiles simultaneously and thereby improve the difficulty in seldom used appliance profiling.

Another interesting future path would collect additional data more directly representing human behavior. Humans are the most influential impact factor and hence occupancy, current well-being, family planners and attitudes towards smart home topics form highly interesting data sources that might further close the gap in accuracy between predictions and the ground truth. All research from how to collect this data up to its impact and predictability would significantly contribute to appliance level load applications.

7 Conclusion

This paper examines various deep learning architectures along with important feature groups for appliance level load prediction. It shows that deep learning consistently provides more accurate predictions than tree-based and multistep SVR benchmarks. The contributions of the paper are twofold. First, the study demonstrates the robustness of the LSTM network across different data sets and appliance types. Secondly, it identifies cyclical encoded time features as a highly important feature group alongside weather features to enhance prediction performance. The findings

additionally contribute to the distinct usage of time features in sequential forecasters demonstrating the positive impact of cyclical encoding.

References

- European Commission. Eurobarometer survey: Europeans consider climate change to be the most serious problem facing the world, 2021. URL https://ec.europa.eu/commission/presscorner/detail/en/ip_21_3156.
- International Energy Agency. Intelligent efficiency – a case study of barriers and solutions – smart homes, March 2018. URL https://www.iea-4e.org/wp-content/uploads/publications/2018/03/Case_Study_HEMS_Final_Report.pdf.
- A. Capasso, W. Grattieri, R. Lamedica, and A. Prudenzi. A bottom-up approach to residential load modeling. *IEEE Transactions on Power Systems*, 9(2):957–964, May 1994. ISSN 1558-0679. doi: 10.1109/59.317650. Conference Name: IEEE Transactions on Power Systems.
- Jukka V. Paatero and Peter D. Lund. A model for generating household electricity load profiles. *International Journal of Energy Research*, 30(5), 2006. ISSN 1099-114X. doi: 10.1002/er.1136. URL <https://onlinelibrary.wiley.com/doi/abs/10.1002/er.1136>.
- Yuan Jin, Jieyan Xu, Da Yan, Hongsan Sun, Jingjing An, Jianghui Tang, and Ruosi Zhang. Appliance use behavior modelling and evaluation in residential buildings: A case study of television energy use. *Building Simulation*, 13, June 2020. doi: 10.1007/s12273-020-0648-8.
- Bingtuan Gao, Xiaofeng Liu, and Zhenyu Zhu. A bottom-up model for household load profile based on the consumption behavior of residents. *Energies*, 11(8), 2018. ISSN 1996-1073. doi: 10.3390/en11082112. URL <https://www.mdpi.com/1996-1073/11/8/2112>.
- Yuting Ji, Elizabeth Buechler, and Ram Rajagopal. Data-driven load modeling and forecasting of residential appliances. *IEEE Transactions on Smart Grid*, 11(3):2652–2661, 2020. doi: 10.1109/TSG.2019.2959770.
- Shailendra Singh and Abdulsalam Yassine. Big data mining of energy time series for behavioral analytics and energy consumption forecasting. *Energies*, 11(2), 2018. doi: 10.3390/en11020452. URL <https://www.mdpi.com/1996-1073/11/2/452>.
- IH Laouali, H Qassemi, M Marzouq, A Ruano, SB Dosse, and H El Fadili. A non linear autoregressive neural network model for forecasting appliance power consumption. *Lecture Notes in Electrical Engineering, Springer*, 2022. doi: 10.1007/978-981-33-6893-4_69.
- Tareq Hossen, Arun Sukumaran Nair, Sima Noghanian, and Prakash Ranganathan. Optimal Operation of Smart Home Appliances using Deep Learning. In *2018 North American Power Symposium (NAPS)*, pages 1–6, 2018. doi: 10.1109/NAPS.2018.8600674.
- David Lachut, Nilanjan Banerjee, and Sami Rollins. Predictability of energy use in homes. In *International Green Computing Conference*, pages 1–10, November 2014. doi: 10.1109/IGCC.2014.7039146.
- Mina Razghandi and Damla Turgut. Residential appliance-level load forecasting with deep learning. pages 1–6, 2020a. doi: 10.1109/GLOBECOM42002.2020.9348197.
- Mina Razghandi, Hao Zhou, Melike Erol-Kantarci, and Damla Turgut. Smart home energy management: Sequence-to-sequence load forecasting and q-learning. *arXiv*, 2021a. URL <https://arxiv.org/abs/2109.12440v1>.
- Mina Razghandi, Hao Zhou, Melike Erol-Kantarci, and Damla Turgut. Short-Term Load Forecasting for Smart HomeAppliances with Sequence to Sequence Learning. *arXiv:2106.15348 [cs, eess]*, 2021b. URL <http://arxiv.org/abs/2106.15348>. arXiv: 2106.15348.
- Christoph Bandt and Bernd Pompe. Permutation entropy: a natural complexity measure for time series. *Physical review letters*, 88 17:174102, 2002.
- Andre L.L. Aquino, Heitor S. Ramos, Alejandro C. Frery, Leonardo P. Viana, Tamer S.G. Cavalcante, and Osvaldo A. Rosso. Characterization of electric load with information theory quantifiers. *Physica A: Statistical Mechanics and its Applications*, 465:277–284, 2017. ISSN 0378-4371. doi: <https://doi.org/10.1016/j.physa.2016.08.017>. URL <https://www.sciencedirect.com/science/article/pii/S0378437116305337>.
- Bilal Fadlallah, BD Chen, Andreas Keil, and Jose Principe. Weighted-permutation entropy: A complexity measure for time series incorporating amplitude information. *Physical review. E, Statistical, nonlinear, and soft matter physics*, 87:022911, February 2013. doi: 10.1103/PhysRevE.87.022911.
- Maik Riedl, Andreas Müller, and Niels Wessel. Practical considerations of permutation entropy: A tutorial review. *The European Physical Journal Special Topics*, 222, 06 2013. doi: 10.1140/epjst/e2013-01862-7.

- Luis M. Candanedo, Véronique Feldheim, and Dominique Deramaix. Data driven prediction models of energy use of appliances in a low-energy house. *Energy and Buildings*, 140:81–97, April 2017. ISSN 0378-7788. doi: 10.1016/j.enbuild.2017.01.083. URL <https://www.sciencedirect.com/science/article/pii/S0378778816308970>.
- Shahida Khatoon, Ibraheem, Arunesh Kr. Singh, and Priti. Effects of various factors on electric load forecasting: An overview. In *2014 6th IEEE Power India International Conference (PIICON)*, pages 1–5, 2014. doi: 10.1109/POWERI.2014.7117763.
- Luis Hernandez, Carlos Baladrón, Javier M. Aguiar, Belén Carro, Antonio J. Sanchez-Esguevillas, and Jaime Lloret. Short-term load forecasting for microgrids based on artificial neural networks. *Energies*, 6(3):1385–1408, 2013. ISSN 1996-1073. doi: 10.3390/en6031385. URL <https://www.mdpi.com/1996-1073/6/3/1385>.
- M. Ramezani, H. Falaghi, M.-R. Haghifam, and G.A. Shahryari. Short-term electric load forecasting using neural networks. In *EUROCON 2005 - The International Conference on "Computer as a Tool"*, volume 2, pages 1525–1528, 2005. doi: 10.1109/EURCON.2005.1630255.
- Tim Unterluggauer, Kalle Rauma, Pertti Järventausta, and Christian Rehtanz. Short-term load forecasting at electric vehicle charging sites using a multivariate multi-step long short-term memory: A case study from finland. *IET Electrical Systems in Transportation*, 11(4):405–419, 2021. doi: <https://doi.org/10.1049/els2.12028>. URL <https://ietresearch.onlinelibrary.wiley.com/doi/abs/10.1049/els2.12028>.
- Yujia He, Janosch Henze, and Bernhard Sick. Forecasting power grid states for regional energy markets with deep neural networks. In *2020 International Joint Conference on Neural Networks (IJCNN)*, pages 1–8, 2020. doi: 10.1109/IJCNN48605.2020.9207536.
- Ljubisa Sehovac and Katarina Grolinger. Deep learning for load forecasting: Sequence to sequence recurrent neural networks with attention. *IEEE Access*, 8:36411–36426, 2020a. doi: 10.1109/ACCESS.2020.2975738.
- Salah Bouktif, Ali Fiaz, Ali Ouni, and Mohamed Adel Serhani. Optimal deep learning lstm model for electric load forecasting using feature selection and genetic algorithm: Comparison with machine learning approaches †. *Energies*, 11(7), 2018. ISSN 1996-1073. doi: 10.3390/en11071636. URL <https://www.mdpi.com/1996-1073/11/7/1636>.
- Maria Sinimaa, Margarita Spichakova, Juri Belikov, and Eduard Petlenkov. Feature engineering of weather data for short-term energy consumption forecast. In *2021 IEEE Madrid PowerTech*, pages 1–6, 2021. doi: 10.1109/PowerTech46648.2021.9494920.
- Margarita Spichakova, Juri Belikov, Kalvi Nõu, and Eduard Petlenkov. Feature engineering for short-term forecast of energy consumption. In *2019 IEEE PES Innovative Smart Grid Technologies Europe (ISGT-Europe)*, pages 1–5, 2019. doi: 10.1109/ISGTEurope.2019.8905698.
- Neelam Mughees, Syed Ali Mohsin, Abdullah Mughees, and Anam Mughees. Deep sequence to sequence bi-lstm neural networks for day-ahead peak load forecasting. *Expert Systems with Applications*, 175:114844, 2021a. ISSN 0957-4174. doi: <https://doi.org/10.1016/j.eswa.2021.114844>. URL <https://www.sciencedirect.com/science/article/pii/S0957417421002852>.
- Lechen Li, Christoph J. Meinrenken, Vijay Modi, and Patricia J. Culligan. Short-term apartment-level load forecasting using a modified neural network with selected auto-regressive features. *Applied Energy*, 287:116509, 2021. ISSN 0306-2619. doi: <https://doi.org/10.1016/j.apenergy.2021.116509>. URL <https://www.sciencedirect.com/science/article/pii/S0306261921000672>.
- Dominique Smith, Kristen Jaskie, John Cadigan, Joseph Marvin, and Andreas Spanias. Machine Learning For Fast Short-Term Energy Load Forecasting. In *2020 IEEE Conference on Industrial Cyberphysical Systems (ICPS)*, volume 1, pages 433–436, June 2020. doi: 10.1109/ICPS48405.2020.9274781.
- Abdul Wahab, Muhammad Anas Tahir, Naveed Iqbal, Adnan Ul-Hasan, Faisal Shafait, and Syed Muhammad Raza Kazmi. A novel technique for short-term load forecasting using sequential models and feature engineering. *IEEE Access*, 9:96221–96232, 2021. doi: 10.1109/ACCESS.2021.3093481.
- Vitor Cerqueira, Nuno Moniz, and Carlos Soares. Vest: Automatic feature engineering for forecasting. *arXiv:2010.07137 [cs, stat]*, 2020. URL <http://arxiv.org/abs/2010.07137>. arXiv: 2010.07137.
- Mina Razghandi and Damla Turgut. Residential Appliance-Level Load Forecasting with Deep Learning. In *GLOBE-COM 2020 - 2020 IEEE Global Communications Conference*, pages 1–6, 2020b. doi: 10.1109/GLOBECOM42002.2020.9348197. ISSN: 2576-6813.
- Irislav Drezga and Saifur Rahman. Input variable selection for ann-based short-term load forecasting. *IEEE Transactions on Power Systems*, 13:1238–1244, 1998.

- Syed Ahsin Ali Shah, Wajid Aziz, Malik Sajjad Ahmed Nadeem, Majid Almarashi, Seong-O. Shim, Turki M. Habeebullah, and Cristian Mateos. A novel phase space reconstruction- (psr-) based predictive algorithm to forecast atmospheric particulate matter concentration. *Sci. Program.*, 2019, January 2019. ISSN 1058-9244. doi: 10.1155/2019/6780379. URL <https://doi.org/10.1155/2019/6780379>.
- Elizabeth Bradley and Holger Kantz. Nonlinear time-series analysis revisited. *Chaos: An Interdisciplinary Journal of Nonlinear Science*, 25(9):097610, September 2015. ISSN 1089-7682. doi: 10.1063/1.4917289. URL <http://dx.doi.org/10.1063/1.4917289>.
- Wenyu Zhang, Jinxing Che, Jianzhou Wang, and Jinzhao Liang. Short-term load forecasting by integration of phase space reconstruction, support vector regression and parameter tuning system. In *2008 International Seminar on Future Information Technology and Management Engineering*, pages 402–405, 2008. doi: 10.1109/FITME.2008.35.
- Guo-Feng Fan, Li-Ling Peng, and Wei-Chiang Hong. Short term load forecasting based on phase space reconstruction algorithm and bi-square kernel regression model. *Applied Energy*, 224:13–33, 2018. ISSN 0306-2619. doi: <https://doi.org/10.1016/j.apenergy.2018.04.075>. URL <https://www.sciencedirect.com/science/article/pii/S0306261918306238>.
- Tian Shi, Fei Mei, Jixiang Lu, Jinjun Lu, Yi Pan, Cheng Zhou, Jianzhang Wu, and Jianyong Zheng. Phase space reconstruction algorithm and deep learning-based very short-term bus load forecasting. *Energies*, 12(22), 2019. ISSN 1996-1073. doi: 10.3390/en12224349. URL <https://www.mdpi.com/1996-1073/12/22/4349>.
- Floris Takens. (Taken Embedding) Detecting strange attractors in turbulence. In David Rand and Lai-Sang Young, editors, *Dynamical Systems and Turbulence, Warwick 1980*, Lecture Notes in Mathematics, pages 366–381, Berlin, Heidelberg, 1981. Springer. ISBN 978-3-540-38945-3. doi: 10.1007/BFb0091924.
- Jeremy P. Huke. Embedding nonlinear dynamical systems: A guide to takens’ theorem. 2006.
- Sepp Hochreiter and Jürgen Schmidhuber. Long short-term memory. *Neural computation*, 9:1735–80, December 1997. doi: 10.1162/neco.1997.9.8.1735.
- Alex Graves, Santiago Fernández, and Jürgen Schmidhuber. Bidirectional lstm networks for improved phoneme classification and recognition. pages 799–804, 2005.
- Neelam Mughees, Syed Ali Mohsin, Abdullah Mughees, and Anam Mughees. Deep sequence to sequence Bi-LSTM neural networks for day-ahead peak load forecasting. *Expert Systems with Applications*, 175:114844, 2021b. ISSN 0957-4174. doi: 10.1016/j.eswa.2021.114844.
- Christopher Olah. Understanding lstm networks, August 2015a. URL <https://colah.github.io/posts/2015-08-Understanding-LSTMs/>. [Online; last visited 04-April-2022].
- Christopher Olah. Neural networks, types, and functional programming, September 2015b. URL <https://colah.github.io/posts/2015-09-NN-Types-FP/>. [Online; last visited 04-April-2022].
- Ilya Sutskever, Oriol Vinyals, and Quoc V Le. Sequence to sequence learning with neural networks. In Z. Ghahramani, M. Welling, C. Cortes, N. Lawrence, and K. Q. Weinberger, editors, *Advances in Neural Information Processing Systems*, volume 27. Curran Associates, Inc., 2014. URL <https://proceedings.neurips.cc/paper/2014/file/a14ac55a4f27472c5d894ec1c3c743d2-Paper.pdf>.
- Shengdong Du, Tianrui Li, and Shi-Jinn Horng. Time series forecasting using sequence-to-sequence deep learning framework. In *2018 9th International Symposium on Parallel Architectures, Algorithms and Programming (PAAP)*, pages 171–176, 2018. doi: 10.1109/PAAP.2018.00037.
- Ljubisa Sehovac and Katarina Grolinger. Deep Learning for Load Forecasting: Sequence to Sequence Recurrent Neural Networks With Attention. *IEEE Access*, 8:36411–36426, 2020b. ISSN 2169-3536. doi: 10.1109/ACCESS.2020.2975738. Conference Name: IEEE Access.
- Alessandro Angioi. Time series forecasting with an lstm encoder/decoder in tensorflow 2.0, February 2020. URL <https://www.angioi.com/time-series-encoder-decoder-tensorflow/>. [Online; posted 03-February-2020].
- Ian Goodfellow, Yoshua Bengio, and Aaron Courville. *Deep Learning*. MIT Press, 2016. <http://www.deeplearningbook.org>.
- Y. LeCun, B. Boser, J. S. Denker, D. Henderson, R. E. Howard, W. Hubbard, and L. D. Jackel. Backpropagation applied to handwritten zip code recognition. *Neural Computation*, 1(4):541–551, 1989. doi: 10.1162/neco.1989.1.4.541.

- Kasun Amarasinghe, Daniel L. Marino, and Milos Manic. Deep neural networks for energy load forecasting. In *2017 IEEE 26th International Symposium on Industrial Electronics (ISIE)*, pages 1483–1488, 2017. doi: 10.1109/ISIE.2017.8001465. ISSN: 2163-5145.
- Ke Yan, Xudong Wang, Yang Du, Ning Jin, Haichao Huang, and Hangxia Zhou. Multi-Step Short-Term Power Consumption Forecasting with a Hybrid Deep Learning Strategy. *Energies*, 11(11):3089, 2018. doi: 10.3390/en11113089. URL <https://www.mdpi.com/1996-1073/11/11/3089>. Number: 11 Publisher: Multidisciplinary Digital Publishing Institute.
- Tianqi Chen and Carlos Guestrin. Xgboost: A scalable tree boosting system. *CoRR*, abs/1603.02754, 2016. URL <http://arxiv.org/abs/1603.02754>.
- Yukun Bao, Tao Xiong, and Zhongyi Hu. Multi-step-ahead time series prediction using multiple-output support vector regression. *Neurocomputing*, 129:482–493, 2014. ISSN 0925-2312. doi: 10.1016/j.neucom.2013.09.010. URL <https://www.sciencedirect.com/science/article/pii/S092523121300917X>.
- Fernando Pérez-Cruz, Gustau Camps-Valls, Emilio Olivas, Juan Perez-Ruixo, Aníbal Figueiras-Vidal, and Antonio Artés Rodríguez. Multi-dimensional function approximation and regression estimation. pages 757–762, August 2002. ISBN 978-3-540-44074-1. doi: 10.1007/3-540-46084-5_123.
- Stephen Makonin, Bradley Ellert, Ivan V. Bajic, and Fred Popowich. Electricity, water, and natural gas consumption of a residential house in canada from 2012 to 2014. *Scientific Data*, 3(1), 2016.
- David Murray, Lina Stanković, and Vladimir Stanković. An electrical load measurements dataset of united kingdom households from a two-year longitudinal study. *Scientific Data*, 4, 2017.
- Andrea Monacchi, Dominik Egarter, Wilfried Elmenreich, Salvatore D’Alessandro, and Andrea M. Tonello. Greend: An energy consumption dataset of households in italy and austria. In *2014 IEEE International Conference on Smart Grid Communications (SmartGridComm)*, pages 511–516, 2014. doi: 10.1109/SmartGridComm.2014.7007698.
- Oliver Parson, Grant Fisher, April Hersey, Nipun Batra, Jack Kelly, Amarjeet Singh, William Knottenbelt, and Alex Rogers. Dataport and nilmtk: A building data set designed for non-intrusive load monitoring. In *2015 IEEE Global Conference on Signal and Information Processing (GlobalSIP)*, pages 210–214, 2015. doi: 10.1109/GlobalSIP.2015.7418187.
- Rob J. Hyndman and Anne B. Koehler. Another look at measures of forecast accuracy. *International Journal of Forecasting*, 22(4):679–688, 2006. ISSN 0169-2070. doi: <https://doi.org/10.1016/j.ijforecast.2006.03.001>. URL <https://www.sciencedirect.com/science/article/pii/S0169207006000239>.
- Kaiyu Sun and Tianzhen Hong. A framework for quantifying the impact of occupant behavior on energy savings of energy conservation measures. *Energy and Buildings*, 146:383–396, 2017. ISSN 0378-7788. doi: <https://doi.org/10.1016/j.enbuild.2017.04.065>. URL <https://www.sciencedirect.com/science/article/pii/S0378778817302013>.
- Guillaume Tausin, Umberto Lupo, Lewis Tunstall, Julian Burella Pérez, Matteo Caorsi, Anibal Medina-Mardones, Alberto Dassatti, and Kathryn Hess. giotto-tda: A topological data analysis toolkit for machine learning and data exploration, 2020.

Appendices

A Parameters

A.1 Predictability and Feature Parameters

Table A.1: Predictability and Feature Parameters

parameters	setting	software (packages)
order: 7 delay: 1 normalize: False	weighted permutation entropy	pyentrp
time_delay: 1 dimension: 2 flatten: True	Taken embedding	giotto-tda [Tausin et al., 2020]

A.2 Model Parameters

Table A.2: Model Parameters

Parameters	Model	Dataset	software (packages)
epochs: 10 neurons per layer: 172 activation: leaky rectified linear unit alpha: 0.2 loss: mean squared error optimizer: adam learning rate: $1e^{-4}$ seeds: [42, 10, 567, 239, 400, 1390, 380, 9, 27, 769]	default	all	TensorFlow
boosting iterations: 750	XGBoost	all	xgb (GPU Support)
gamma: $1/(\text{feature count} * \text{variance of training data})$ degree: 2 C: 0.1	MSVR	all	Implementation of papaer by authors (https://github.com/Analytics-for-Forecasting/msvr)
layers: 2 drop out rate: 0.06	LSTM/BiLSTM	REFIT, GREEND, PecanSD	TensorFlow
neurons per layer: 281 drop out rate: 0.13 learning rate: $5e^{-4}$ alpha: 0.5	LSTM/BiLSTM	AMPds2	TensorFlow
learning rate: $1e^{-3}$ epochs: 100	decoder 1 in S2S reversed	all	tensorflow (reproduced based on information from paper)
neurons per layer: 377	S2S context	all	TensorFlow
neurons per layer: 182 dropout rate: 0.17	FFNN	REFIT, GREEND, PecanSD	TensorFlow
neurons per layer: 281	FFNN	AMPds2	tensorflow
layers CNN: 2 convolutional filter size: 64 neurons per layer LSTM: 146 dropout rate: 0.36 max pooling size: 2 kernel size: 2	CNN-LSTM	all	TensorFlow

Tuning Options for Hyperparameters

Parameters	Model	Dataset	software (packages)
layers range: [1, 5] neurons per layer range: [1, 400] batch size choice: [8, 16, 32, 64, 128] learning rate range: [0.0001, 0.5] dropout rate range: [0.01, 0.5] alpha for activation choice: [0.1, 0.2, 0.5]	LSTM/BiLSTM, S2S, FFNN, CNN-LSTM	all	TensorFlow
gamma range: [1/100, 1/1000, 1 / (X_train.shape[1] * X_train.var())] epsilon range: [1, 0.0001] C range: [100, 0.001]	MSVR		manual setup

Tuning for deep learning architectures used 25-fold cross validation and 20 epochs in a random search procedure. Each newly found Hyperparameter set was compared against the best performing set for the LSTM model on REFIT. If it performed worse, the LSTM-default Parameter Setting was used.

Table B.1: Results for Fridge on All Datasets

Dataset	Models															
Features	XGBoost				MSVR				LSTM				BiLSTM			
	RMSE	nRMSE	Acc		RMSE	nRMSE	Acc		RMSE	nRMSE	Acc		RMSE	nRMSE	Acc	
GREEND	RMSE	nRMSE	Acc	RMSE	nRMSE	Acc	RMSE	nRMSE	Acc	RMSE	nRMSE	Acc	RMSE	nRMSE	Acc	RMSE
base	23.40	0.1876	0.55	22.17	0.1778	0.57	22.01	0.1765	0.58	22.08	0.1771	0.59	22.14	0.1775	0.52	22.10
date-time	23.67	0.1899	0.49	22.33	0.1790	0.59	22.86	0.1833	0.73	22.62	0.1814	0.72	22.22	0.1782	0.54	23.53
weather	24.09	0.1932	0.43	21.62	0.1734	0.53	21.32	0.1710	0.59	21.39	0.1716	0.57	21.77	0.1746	0.53	21.69
appl.	23.14	0.1856	0.51	21.93	0.1758	0.53	21.65	0.1736	0.60	21.64	0.1736	0.59	22.00	0.1764	0.48	21.69
ls-on/off	23.40	0.1876	0.55	22.18	0.1779	0.57	21.98	0.1763	0.58	22.07	0.1770	0.60	22.07	0.1770	0.52	21.97
autoreg.	22.98	0.1843	0.49	21.98	0.1762	0.60	21.85	0.1752	0.59	21.91	0.1757	0.60	22.01	0.1765	0.52	21.78
interact.	23.59	0.1892	0.47	22.20	0.1780	0.50	22.01	0.1765	0.56	22.11	0.1773	0.53	22.00	0.1764	0.49	23.07
VEST	25.06	0.2010	0.43	22.10	0.1772	0.61	22.37	0.1794	0.60	22.40	0.1797	0.60	n.d.	n.d.	n.d.	22.16
ps	n.d.	n.d.	n.d.	n.d.	n.d.	n.d.	23.88	0.1915	0.62	22.02	0.1766	0.58	n.d.	n.d.	n.d.	n.d.
all	24.38	0.1956	0.46	21.67	0.1738	0.56	24.41	0.1958	0.61	22.45	0.1800	0.57	22.11	0.1773	0.49	25.99
w+dt	24.43	0.1959	0.46	21.93	0.1759	0.57	22.39	0.1795	0.69	22.17	0.1778	0.69	22.16	0.1777	0.54	24.78
PecanSD	RMSE	nRMSE	Acc	RMSE	nRMSE	Acc	RMSE	nRMSE	Acc	RMSE	nRMSE	Acc	RMSE	nRMSE	Acc	RMSE
base	25.67	0.1879	0.44	22.86	0.1673	0.44	23.52	0.1722	0.47	23.23	0.1700	0.43	22.97	0.1681	0.49	23.27
date-time	23.79	0.1741	0.46	22.02	0.1612	0.38	22.37	0.1637	0.48	22.59	0.1653	0.39	23.14	0.1694	0.57	22.96
weather	24.60	0.1801	0.46	22.49	0.1646	0.53	23.18	0.1697	0.60	23.10	0.1691	0.57	22.76	0.1666	0.53	22.99
appl.	24.36	0.1783	0.42	22.58	0.1653	0.44	23.26	0.1703	0.50	22.95	0.1680	0.47	22.71	0.1662	0.50	23.02
ls-on/off	25.67	0.1879	0.44	22.82	0.1670	0.46	23.55	0.1724	0.48	23.28	0.1704	0.44	22.99	0.1683	0.50	23.36
autoreg.	25.36	0.1857	0.44	22.71	0.1662	0.46	24.26	0.1776	0.45	24.31	0.1779	0.49	23.08	0.1690	0.50	23.75
interact	24.87	0.1821	0.46	22.54	0.1650	0.43	23.05	0.1688	0.51	22.72	0.1663	0.54	22.78	0.1668	0.49	22.63
VEST	25.82	0.1890	0.38	22.50	0.1647	0.41	23.10	0.1691	0.47	23.12	0.1693	0.48	n.d.	n.d.	n.d.	23.18
ps	n.d.	n.d.	n.d.	n.d.	n.d.	n.d.	23.61	0.1729	0.51	22.66	0.1659	0.45	n.d.	n.d.	n.d.	n.d.
all	23.78	0.1741	0.44	23.15	0.1695	0.30	23.51	0.1721	0.52	23.11	0.1692	0.48	23.01	0.1685	0.51	24.13
w+dt	23.50	0.1720	0.49	22.09	0.1617	0.55	22.96	0.1681	0.64	22.80	0.1669	0.58	22.94	0.1679	0.57	23.29
REFIT	RMSE	nRMSE	Acc	RMSE	nRMSE	Acc	RMSE	nRMSE	Acc	RMSE	nRMSE	Acc	RMSE	nRMSE	Acc	RMSE
base	17.64	0.1742	0.80	15.72	0.1552	0.78	16.02	0.1582	0.77	15.94	0.1574	0.77	15.81	0.1561	0.77	15.92
date-time	17.41	0.1719	0.79	15.91	0.1571	0.76	16.02	0.1582	0.75	15.92	0.1572	0.76	15.72	0.1553	0.77	15.78
weather	17.09	0.1688	0.81	15.86	0.1567	0.77	16.01	0.1581	0.76	15.91	0.1571	0.76	15.78	0.1558	0.77	15.85
appl.	17.77	0.1755	0.81	16.11	0.1591	0.77	16.19	0.1599	0.76	16.04	0.1584	0.77	15.86	0.1566	0.78	16.09
ls-on/off	17.84	0.1762	0.80	16.09	0.1589	0.77	16.02	0.1582	0.77	15.98	0.1579	0.77	15.86	0.1566	0.78	16.00
autoreg.	17.32	0.1711	0.80	16.01	0.1582	0.77	16.18	0.1598	0.76	16.06	0.1586	0.77	15.88	0.1568	0.77	16.02
interact.	17.84	0.1762	0.80	16.13	0.1593	0.77	15.97	0.1577	0.78	16.00	0.1581	0.78	15.89	0.1569	0.78	16.08
VEST	17.30	0.1708	0.80	15.84	0.1565	0.77	15.96	0.1577	0.76	16.00	0.1580	0.76	n.d.	n.d.	n.d.	15.98
ps	n.d.	n.d.	n.d.	n.d.	n.d.	n.d.	15.89	0.1569	0.77	15.96	0.1576	0.77	n.d.	n.d.	n.d.	n.d.
all	17.65	0.1743	0.80	16.19	0.1599	0.77	16.28	0.1608	0.77	16.15	0.1595	0.77	15.99	0.1579	0.77	17.09
w+dt	17.09	0.1688	0.80	15.88	0.1568	0.76	16.10	0.1590	0.75	16.02	0.1582	0.76	15.73	0.1554	0.77	15.92
AMPds2	RMSE	nRMSE	Acc	RMSE	nRMSE	Acc	RMSE	nRMSE	Acc	RMSE	nRMSE	Acc	RMSE	nRMSE	Acc	RMSE
base	25.61	0.1350	0.44	22.68	0.1195	0.51	22.54	0.1188	0.56	22.38	0.1180	0.57	22.52	0.1187	0.59	22.50
date-time	24.47	0.1290	0.50	22.31	0.1176	0.55	22.52	0.1187	0.58	22.39	0.1180	0.58	22.42	0.1182	0.59	22.41
weather	27.97	0.1474	0.44	22.72	0.1198	0.53	22.76	0.1200	0.56	22.75	0.1199	0.55	22.53	0.1188	0.61	22.63
appl.	24.91	0.1313	0.46	22.74	0.1199	0.49	22.59	0.1191	0.55	22.38	0.1180	0.56	22.49	0.1186	0.59	22.43
ls-on/off	25.61	0.1350	0.44	22.64	0.1193	0.51	22.61	0.1192	0.56	22.36	0.1179	0.58	22.52	0.1187	0.58	22.47
autoreg.	24.89	0.1312	0.47	22.53	0.1188	0.52	22.56	0.1189	0.56	22.29	0.1175	0.57	22.46	0.1184	0.60	22.47
interact	25.53	0.1346	0.46	22.65	0.1194	0.50	22.86	0.1205	0.54	22.58	0.1190	0.56	22.44	0.1183	0.59	22.38
VEST	24.69	0.1301	0.48	22.61	0.1192	0.51	22.52	0.1187	0.58	22.39	0.1180	0.58	n.d.	n.d.	n.d.	22.49
ps	n.d.	n.d.	n.d.	n.d.	n.d.	n.d.	22.68	0.1195	0.55	22.38	0.1180	0.58	n.d.	n.d.	n.d.	n.d.
all	25.42	0.1340	0.47	22.96	0.1210	0.46	22.74	0.1199	0.57	22.49	0.1185	0.58	22.52	0.1187	0.59	22.72

Table B.2: Results Different Appliances REFTT

Dataset		Models																								
Features		XGBoost			MSVR			LSTM			BiLSTM			Seq2Seq reversed			Seq2Seq context			FFNN			CNN-LSTM			
Dryer		RMSE	nRMSE	Acc	RMSE	nRMSE	Acc	RMSE	nRMSE	Acc	RMSE	nRMSE	Acc	RMSE	nRMSE	Acc	RMSE	nRMSE	Acc	RMSE	nRMSE	Acc	RMSE	nRMSE	Acc	
base		18.64	0.0390	1.00	18.16	0.0380	1.00	18.12	0.0379	1.00	18.12	0.0379	1.00	18.12	0.0379	1.00	18.11	0.0379	1.00	18.12	0.0379	1.00	18.13	0.0380	1.00	
date-time		21.24	0.0445	1.00	18.36	0.0384	1.00	18.45	0.0386	1.00	18.29	0.0383	1.00	18.18	0.0380	1.00	18.14	0.0380	1.00	18.15	0.0380	1.00	18.11	0.0379	1.00	
weather		35.46	0.0742	1.00	18.51	0.0388	1.00	18.68	0.0391	1.00	18.52	0.0388	1.00	18.22	0.0381	1.00	18.55	0.0388	1.00	18.19	0.0381	1.00	18.36	0.0384	1.00	
appl.		27.31	0.0572	1.00	18.33	0.0384	1.00	18.24	0.0382	1.00	18.56	0.0389	1.00	18.12	0.0379	1.00	18.22	0.0381	1.00	18.08	0.0378	1.00	18.43	0.0386	1.00	
ls-on/off		34.39	0.0720	1.00	18.35	0.0384	1.00	18.14	0.0380	1.00	18.11	0.0379	1.00	18.14	0.0380	1.00	18.28	0.0383	1.00	18.43	0.0386	1.00	18.12	0.0379	1.00	
autoreg		21.51	0.0450	1.00	18.38	0.0385	1.00	18.41	0.0385	1.00	18.18	0.0381	1.00	18.14	0.0380	1.00	18.27	0.0382	1.00	18.12	0.0379	1.00	18.13	0.0380	1.00	
interact.		27.57	0.0577	1.00	18.32	0.0384	1.00	18.40	0.0385	1.00	18.59	0.0389	1.00	18.12	0.0379	1.00	18.28	0.0383	1.00	18.13	0.0380	1.00	18.12	0.0379	1.00	
VEST		123.00	0.0481	1.00	18.17	0.0380	1.00	18.10	0.0379	1.00	18.11	0.0379	1.00	n.d.	n.d.	n.d.	18.12	0.0379	1.00	183.88	0.3849	1.00	18.12	0.0379	1.00	
ps		n.d.	n.d.	n.d.	n.d.	n.d.	n.d.	18.13	0.0380	1.00	18.12	0.0379	1.00	n.d.	n.d.	n.d.	n.d.	n.d.	18.12	0.0379	1.00	18.13	0.0379	1.00	1.00	
all		38.07	0.0797	1.00	18.49	0.0387	1.00	20.29	0.0425	1.00	18.36	0.0384	1.00	18.59	0.0389	1.00	19.72	0.0413	1.00	18.20	0.0381	1.00	18.19	0.0381	1.00	
w+dt		36.52	0.0765	1.00	18.47	0.0387	1.00	18.85	0.0395	1.00	18.86	0.0395	1.00	18.60	0.0389	1.00	18.39	0.0385	1.00	18.22	0.0382	1.00	18.33	0.0384	1.00	
Dishw.		RMSE	nRMSE	Acc	RMSE	nRMSE	Acc	RMSE	nRMSE	Acc	RMSE	nRMSE	Acc	RMSE	nRMSE	Acc	RMSE	nRMSE	Acc	RMSE	nRMSE	Acc	RMSE	nRMSE	Acc	
base		105.53	0.1042	0.97	99.39	0.0982	0.97	99.44	0.0982	0.97	99.38	0.0982	0.97	99.44	0.0982	0.97	99.47	0.0983	0.97	99.42	0.0982	0.97	100.47	0.0992	0.97	
date-time		119.54	0.1181	0.97	98.84	0.0976	0.97	100.32	0.0991	0.97	99.41	0.0982	0.97	99.47	0.0983	0.97	100.31	0.0991	0.97	99.13	0.0979	0.97	99.85	0.0986	0.97	
weather		119.32	0.1179	0.97	99.99	0.0988	0.97	100.93	0.0997	0.97	99.77	0.0986	0.97	99.32	0.0981	0.97	101.09	0.0999	0.97	99.54	0.0983	0.97	101.08	0.0998	0.97	
appl.		112.01	0.1106	0.97	99.16	0.0979	0.97	100.96	0.0997	0.97	100.29	0.0991	0.97	99.68	0.0985	0.97	101.66	0.1004	0.97	99.44	0.0982	0.97	103.48	0.1022	0.97	
ls-on/off		141.37	0.1396	0.97	99.64	0.0984	0.97	100.78	0.0995	0.97	99.75	0.0985	0.97	99.64	0.0984	0.97	101.52	0.1003	0.97	100.33	0.0991	0.97	99.77	0.0986	0.97	
autoreg.		117.45	0.1160	0.97	99.12	0.0979	0.97	99.72	0.0985	0.97	99.17	0.0980	0.97	99.17	0.0980	0.97	100.09	0.0989	0.97	99.32	0.0981	0.97	99.45	0.0982	0.97	
interact.		120.29	0.1188	0.97	99.10	0.0979	0.97	101.47	0.1002	0.97	100.25	0.0990	0.97	100.69	0.0995	0.97	101.27	0.1000	0.97	99.29	0.0981	0.97	99.91	0.0987	0.97	
VEST		117.07	0.1156	0.97	99.48	0.0983	0.97	99.53	0.0983	0.97	99.44	0.0982	0.97	n.d.	n.d.	n.d.	99.52	0.0983	0.97	131.42	0.1298	0.97	99.61	0.0984	0.97	
ps		n.d.	n.d.	n.d.	n.d.	n.d.	n.d.	99.44	0.0982	0.97	99.39	0.0982	0.97	n.d.	n.d.	n.d.	n.d.	n.d.	99.43	0.0982	0.97	99.72	0.0985	0.97	1.00	
all		123.18	0.1217	0.97	99.36	0.0981	0.97	105.07	0.1038	0.97	99.69	0.0985	0.97	100.20	0.0990	0.97	102.39	0.1011	0.97	99.66	0.0984	0.97	99.36	0.0981	0.97	
w+dt		123.75	0.1222	0.97	99.48	0.0983	0.97	104.23	0.1030	0.97	101.66	0.1004	0.97	99.85	0.0986	0.97	104.19	0.1029	0.97	99.60	0.0984	0.97	101.51	0.1003	0.97	
WM		RMSE	nRMSE	Acc	RMSE	nRMSE	Acc	RMSE	nRMSE	Acc	RMSE	nRMSE	Acc	RMSE	nRMSE	Acc	RMSE	nRMSE	Acc	RMSE	nRMSE	Acc	RMSE	nRMSE	Acc	
base		102.78	0.0456	0.93	96.03	0.0426	0.94	96.26	0.0427	0.94	96.16	0.0426	0.94	96.32	0.0427	0.94	96.24	0.0427	0.94	96.42	0.0427	0.94	96.62	0.0428	0.94	
date-time		101.67	0.0451	0.93	95.47	0.0423	0.94	96.39	0.0427	0.94	95.82	0.0425	0.94	95.82	0.0425	0.94	96.40	0.0427	0.94	95.74	0.0424	0.94	96.29	0.0427	0.94	
weather		102.68	0.0455	0.93	95.63	0.0424	0.94	96.24	0.0427	0.94	95.88	0.0425	0.94	95.81	0.0425	0.94	96.11	0.0426	0.94	95.81	0.0425	0.94	97.26	0.0431	0.94	
appl.		100.56	0.0446	0.94	95.13	0.0422	0.94	95.82	0.0425	0.94	95.34	0.0423	0.94	96.31	0.0427	0.94	96.12	0.0426	0.94	95.62	0.0424	0.94	96.94	0.0430	0.94	
ls-on/off		104.10	0.0461	0.93	96.64	0.0428	0.94	96.66	0.0428	0.94	96.58	0.0428	0.94	96.27	0.0427	0.94	96.40	0.0427	0.94	96.62	0.0428	0.94	96.36	0.0427	0.94	
autoreg.		104.70	0.0464	0.93	95.86	0.0425	0.94	96.28	0.0427	0.94	96.26	0.0427	0.94	96.09	0.0426	0.94	96.12	0.0426	0.94	96.31	0.0427	0.94	96.39	0.0427	0.94	
interact.		102.98	0.0456	0.93	95.43	0.0423	0.94	97.52	0.0432	0.93	96.61	0.0428	0.94	96.64	0.0428	0.94	97.54	0.0432	0.93	95.78	0.0425	0.94	96.29	0.0427	0.94	
VEST		101.73	0.0451	0.93	96.51	0.0428	0.94	96.28	0.0427	0.94	96.21	0.0426	0.94	n.d.	n.d.	n.d.	96.23	0.0427	0.94	584.89	0.2593	0.94	96.54	0.0428	0.94	
ps		n.d.	n.d.	n.d.	n.d.	n.d.	n.d.	96.35	0.0427	0.94	96.26	0.0427	0.94	n.d.	n.d.	n.d.	n.d.	n.d.	96.40	0.0427	0.94	96.66	0.0428	0.94	1.00	
all		108.63	0.0482	0.93	96.33	0.0427	0.94	98.04	0.0435	0.93	96.47	0.0428	0.94	96.59	0.0428	0.94	97.50	0.0432	0.94	96.31	0.0427	0.94	95.82	0.0425	0.94	
w+dt		101.84	0.0451	0.93	95.67	0.0424	0.94	96.99	0.0430	0.93	96.00	0.0426	0.93	96.03	0.0426	0.94	97.49	0.0432	0.93	95.93	0.0425	0.94	96.33	0.0427	0.93	
Telev.		RMSE	nRMSE	Acc	RMSE	nRMSE	Acc	RMSE	nRMSE	Acc	RMSE	nRMSE	Acc	RMSE	nRMSE	Acc	RMSE	nRMSE	Acc	RMSE	nRMSE	Acc	RMSE	nRMSE	Acc	
base		10.44	0.2696	0.94	9.27	0.2394	0.93	9.46	0.2443	0.93	9.48	0.2446	0.93	9.49	0.2448	0.93	9.56	0.2468	0.92	9.38	0.2421	0.92	9.56	0.2468	0.93	
date-time		9.80	0.2529	0.94	9.03	0.2331	0.93	9.41	0.2430	0.93	9.43	0.2433	0.93	9.08	0.2345	0.93	9.52	0.2457	0.92	9.18	0.2368	0.92	9.89	0.2553	0.93	
weather		10.25	0.2645	0.93	9.35	0.2414	0.91	9.64	0.2488	0.92	9.75	0.2517	0.91	9.33	0.2409	0.93	9.71	0.2507	0.92	9.30	0.2400	0.91	9.66	0.2494	0.92	
appl.		10.80	0.2788	0.93	9.54	0.2462	0.91	9.46	0.2442	0.93	9.43	0.2435	0.93	10.02	0.2586	0.90	9.56	0.2467	0.94	9.67	0.2496	0.91	9.81	0.2531	0.94	
ls-on/off		10.13	0.2615	0.93	10.46	0.2700	0.89	10.19	0.2630	0.92	10.01	0.2585	0.92	9.64	0.2487	0.92	10.41	0.2688	0.93	10.63	0.2745	0.89	9.39	0.2423	0.92	
autoreg.		10.03	0.2588	0.93	9.20	0.2374	0.93	9.31	0.2404	0.93	9.35	0.2415	0.93	9.26	0.2390	0.93	9.41	0.2430	0.92	9.34	0.2411	0.91	9.16	0.2364	0.93	
interact.		10.50	0.2711	0.93	9.48	0.2447	0.92	9.73	0.2513	0.93	9.70	0.2503	0.93	9.84	0.2539	0.92	9.99	0.2580	0.93	9.89	0.2552	0.91	9.87	0.2549	0.93	
VEST		10.18	0.2629	0.93	9.42	0.2430	0.92	9.39	0.2423	0.92	9.47	0.2444	0.92	n.d.	n.d.	n.d.	9.53	0.2460	0.92	11.48	0.2964	0.91	9.44	0.2436	0.93	
ps		n.d.	n.d.	n.d.	n.d.	n.d.	n.d.	9.42	0.2433	0.93	9.44	0.2438	0.93	n.d.	n.d.	n.d.	n.d.	n.d.	n.d.	n.d.	9.37	0.2418	0.91	9.54	0.2462	0.93
all		10.51	0.2714	0.94	10.32																					